1506
UNIVERSITÀ
DEGLI STUDI
DI URBINO
CARLO BO

Department of Biomolecular Sciences

Ph.D. PROGRAMME IN: Biomolecular and Health Sciences

CYCLE XXXVII

THESIS TITLE:

CAVEOLIN-1 OVEREXPRESSION ALTERS EXTRACELLULAR VESICLE SECRETION AND CARGO IN AN *IN VITRO* MODEL OF RHABDOMYOSARCOMA: A POSSIBLE LINK TO MALIGNANCY

ACADEMIC DISCIPLINE: BIOS-07/A – BIOCHEMISTRY

Coordinator: Prof. Ferdinando Mannello

Supervisor: Prof. Michele Guescini

Ph.D. student: Rachele Agostini

ACADEMIC YEAR
2023/2024

INDEX

1. BACKGROUND

1.1. Caveolin-1: structural and biological functions

Caveolins are a family of transmembrane proteins localized in specific areas of the phospholipid bilayer called caveolae [1]. The name “caveolae” derives from their shape since they are vesicular invaginations of the plasma membrane around 70 nanometres (nm) in size and by transmission electron microscopy, they seem ‘little caves’. Caveolae are mostly considered to be a subgroup of lipid rafts, which are transmembrane microdomains enriched in specific lipid species residing within the plasma membrane [2–4]; this is not completely true since some proteins are known to belong selectively to either lipid rafts or caveolae but not both [5].

There are three main caveolin isoforms: Caveolin-1 (Cav-1), Caveolin-2 (Cav-2) and Caveolin-3 (Cav-3). Generally speaking, caveolins are small proteins (18-24 kDa).

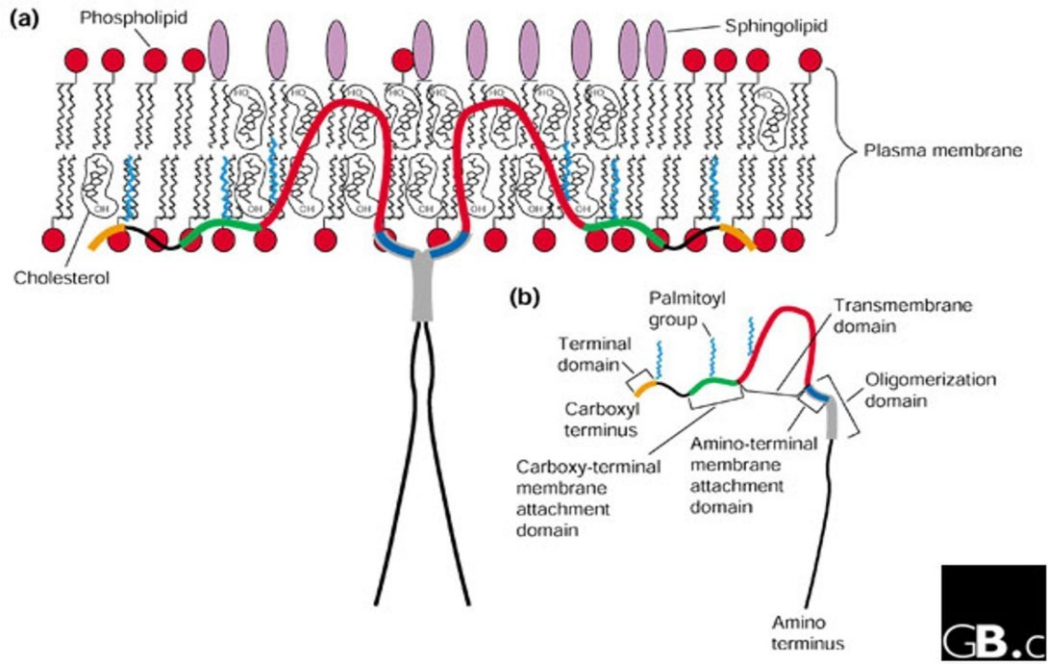

Figure 1. Caveolin-1 primary structure in the phospholipid bilayer and its main domains (picture taken from Williams and Lisanti, 2004 [1])

Cav-1 has a hairpin-like conformation, with N- and C-terminal cytoplasmic tails separated by a transmembrane hydrophobic domain. The two main functional domains of the protein are the tyrosine 14 phosphorylation domain and the oligomerization domain. The two main isoforms of Cav-1 are Cav-1α, the best characterized in terms of function, and Cav-1β (lacking the first 32 aminoacids). Cav-1α can be phosphorylated on tyrosine 14 by Src kinase and on Serine 80 which is demonstrated to regulate Cav-1 and cholesterol trafficking [6,7].

Cav-1 mainly localizes to plasma-membrane caveolae, to the Golgi apparatus and trans-Golgi-derived transport vesicles [8]. It could also exists in a soluble form found in the cytoplasm, as well as a secreted form, depending on the cell type [9]. The first 31 amino acids are crucial in selectively targeting isoforms of Cav-1 to different cellular compartments [10]. Cav-1 is expressed in almost all cell types at different levels: it is mostly represented in adipocytes, endothelial cells, fibroblasts, smooth muscle cells, and a variety of epithelial cells. The expression of Cav-2 goes along with Cav-1, which is also required for the proper membrane localization of Cav-2, while Cav-3 is expressed predominantly in myocytes [11].

Research related to Cav-1 has demonstrated its role in endocytosis (caveolin-mediated endocytosis) [12], exocytosis, signal transduction, vesicular trafficking and cholesterol homeostasis [1].

Many studies have also reported that Cav-1 is directly involved in the process of membrane curvature [13,14]. It can recruit specific lipidic species in its vicinity forming clusters functionalized to stabilize membrane curvature. It directly interacts with charged membrane lipids like phosphatidylserine, and with cholesterol through several interactions in more than one site of the molecule [15]. Indeed, caveolae are known to be much more enriched in cholesterol compared to the neighbouring areas of the phospholipid bilayer, creating a suitable environment for Cav-1 involvement in vesicle formation [16].

1.1.1. Caveolin-1 role in vesicular trafficking

Emerging evidence suggests a novel role for Cav-1 regarding extracellular vesicle (EV) biogenesis and cargo sorting. EVs are small vesicles released by almost all types of cells for cell-to-cell communication, which will be better described in the following sections.

This role directly correlates with Cav-1 localization in the plasma membrane since caveolae and even more lipid rafts are found to be involved in the process of vesiculation [17].

Cav-1 has been detected in exocrine cell derived-secretome [18], like pancreatic acinar cells and also in the EVs released by malignant cells [19]. Some studies have demonstrated that Cav-1 levels in EVs increase after noxious stimuli in a variety of cell types suggesting its ability to enhance EV production [20,21]. Albacete et al. demonstrated that Cav-1 is able to regulate EV biogenesis through the modulation of cholesterol content in the multivesicular bodies (MVBs), the small intracellular vesicles from which a subset of EV takes origin [22].

Furthermore, the EV cargo sorting process is tightly regulated, and it has been found that Cav-1 is involved in it. EVs carry a variety of cellular cargo, including proteins, lipids, DNA, RNA, and small RNA molecules like miRNA. Cav-1 promotes the sorting of specific proteins into the EVs, enhancing the migration and invasiveness of breast cancer cells [23] and it is found to be involved in the selective loading of miRNAs into EVs in response to stimuli, especially oxidative stress [20]. Cav-1 post-translational modifications, such as the previously discussed phosphorylation, play a key role in this process since they promote a change in Cav-1 conformation, allowing it to interact with the molecules responsible for miRNA sorting, like hnRNPA2B [24].

1.1.2. Caveolin-1 and cancer

Current evidence about the role of Cav-1 in cancer does not outline a single type of behaviour by the protein, starting from its contribution in programmed cell death.

The role of Caveolin-1 (Cav-1) in apoptosis is controversial. It has been demonstrated that caveolae are enriched in ceramide, a molecule that induces cell death by inhibiting the PI3-kinase/Akt survival pathway; Cav-1 interacts with PI3-kinase, and its overexpression makes fibroblasts more sensitive to ceramide-induced death through a PI3-kinase-dependent mechanism [25,26]. Cav-1 also promotes apoptosis induced by chemical enhancers in NIH-3T3 fibroblasts and T24 bladder carcinoma [27]. Conversely, caveolae damage induced by cholesterol-sequestering agents has been shown to promote the activation of the PI3-kinase/Akt signalling pathway, indicating that caveolae and Cav-1 are essential for proper survival signalling through this way [28]. Furthermore, it has been shown that overexpression of Cav-1 promotes cell survival by maintaining Akt activation thanks to the inhibition of the serine/threonine protein phosphatases, called PP1 and PP2A [29].

This apparent inconsistency of the pro- or anti-apoptotic role of Cav-1 can be explained by cell-type specific effects and by the cancer stage [30].

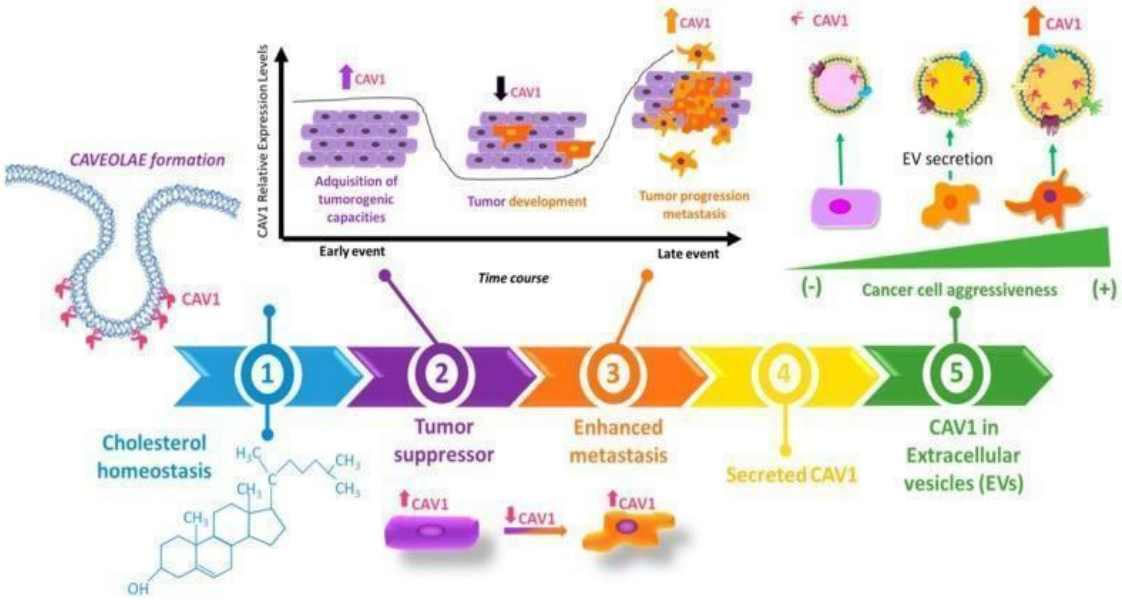

Figure 2. This timeline summarizes the evolution in the discovery of Caveolin-1 functions. (1) Early studies focused on the structural role of Cav-1 and its function in cholesterol transport. (2) Subsequent studies linked Cav-1 to the suppression of oncogenic signalling and correlated the loss of Cav-1 with cell transformation. (3) In later stages of cancer, elevated Cav-1 protein levels are often associated with a metastatic cell phenotype. (4) Cav-1 was later identified as

a secreted protein with "extracellular" functions. (5) Recently, attention has turned to Cav-1 potential roles in extracellular vesicle (EV) mediated cancer aggressiveness. (Picture taken from Campos et al., 2019 [23]).

The first studies related to the involvement of Cav-1 in cancer have shown its tumour-suppressor properties. Indeed, Cav-1 was found to be poorly expressed in many human cancer types such as lung [31], mammary [32], colon [33], ovarian [34], sarcoma [35], including osteosarcoma [36], and glioblastoma [37]. Furthermore, a number of *in vitro* experiments have confirmed the “oncosuppressor” hypothesis. Koleske et al have demonstrated that Cav-1 is downregulated in oncogene-transformed fibroblasts and that this reduction in Cav-1 levels correlates with increased cell proliferation [38].

On the other hand, many studies have demonstrated that Cav-1 expression is positively correlated with tumour growth and metastatic potential [39].

An interesting example to explain the cancer stage-dependent behaviour of Cav-1 is breast cancer. Some studies have demonstrated that Cav-1 acts as a suppressor gene in breast cancer cells, since it is able to inhibit the development of malignant features; other studies have shown that Cav-1 expression promotes breast cancer cell growth and proliferation. In support of the first hypothesis, low or absent levels of Cav-1 mRNA and protein have been detected in tumour tissue samples from human primary breast cancer patients, but also in mouse and *in vitro* models [40]. Furthermore, the re-expression of Cav-1 in transformed breast cancer cell lines led to a decrease in both their cancerous potential and aggressiveness [41,42]. On the other hand, it has been demonstrated that Cav-1 levels are significantly higher in metastatic breast cancer cell lines (MDA-MB-231) compared to the non-metastatic ones (MCF7), and that in breast cancer tissues Cav-1 expression correlated with a higher metastatic potential [43].

A similar scenario has been reported in rhabdomyosarcoma, a soft tissue-derived tumour, in which Cav-1 could represent an indicator of malignancy since its expression correlates with poor differentiation and high proliferation [44]. Human embryonal rhabdomyosarcoma cell lines (RD-cells) represent the *in vitro* model employed in the present study and therefore will be further discussed in the following sections.

Other cancer types in which Cav-1 was found to be involved in the dissemination process are lung cancer [45], clear cell renal carcinoma [46], hepatocellular carcinoma [47], melanoma [48], Ewing sarcoma [49] and many others.

1.2. Rhabdomyosarcoma: overview

Rhabdomyosarcoma (RMS) is a soft tissue malignant tumour arising from mesenchymal cells. It represents the most common soft tissue sarcoma in childhood with about 2.7% of cancer cases among 0-14-year-old children. Overall, the incidence is 4.6 cases per 1 million people younger than 20 years [50].

In general, RMS rises from the loss of the ability to properly differentiate by the mesenchymal cells which are persistently kept in a proliferation state. Four different histological RMS subtypes have been defined by the 2020 WHO (World Health Organization): embryonal, alveolar, spindle cell/sclerosing and pleomorphic [50].

The two most common types are the embryonal (ERMS) and the alveolar (ARMS) ones. In ERMS the chromosome 11p15.5 [51] loses its heterozygosity leading to a variety of consequences among which the hyper-activation of the RAS/ERK pathway [52] is the most relevant one since it plays an important role in the process of tumour growth [53,54], radioresistance [55–57] and metastasis [58]. ARMS is instead characterized by the translocation of t(2;13)(q35;q14) or t(1;13)(q36;q14) chromosome which is responsible for the fusion of the genes PAX3 and 7 with the Forkhead box O1 (FoxO1) that generate the chimeric Pax3-FoxO1 or Pax7-FoxO1 oncoproteins, respectively [59]. Indeed, ERMS is also called fusion-negative RMS, while ARMS is fusion-positive.

Regarding RMS incidence, there is a correlation with the histological subtype: for example, male patients have a higher incidence of embryonal tumours, and black patients of the alveolar one [60].

RMS can occur in every part of the body, but the most common primary sites are head and neck region, genitourinary tract and extremities which often occur in older patients with alveolar histology [61,62]. Other primary sites include the chest wall, perineal/anal

region, and abdomen but they are less common [63]. There are no recognized risk factors for RMS, and it often appears randomly. Suggested predisposition factors regard genetics: Li-Fraumeni cancer susceptibility syndrome (with germline TP53 variants) [64], DICER1 syndrome [65], Neurofibromatosis type I (NF1) [66] but also high birth weight and large size for gestational age for ERMS [67].

Treatment mainly consists of surgery, radio- and chemotherapy which can improve RMS prognosis [68]. The prognosis depends on tumour localization and diffusion: when the primary tumour is not spread yet, patients have a more favourable prognosis receiving combined-modality therapy, with more than 70% of patients surviving 5 years after diagnosis. Relapses often occur in patients with unresectable disease, tumour in an unfavourable site, or metastatic disease at diagnosis. We can summarize the prognosis-related factors as follows: age, site of origin, tumour size, resectability, fusion-positive subtype, metastases at diagnosis, and response to therapy [50].

1.2.1. Caveolin-1 in human rhabdomyosarcoma cell lines (RD)

As briefly introduced before, Cav-1 has a controversial role in cancer disease. Regarding RMS, and particularly the embryonal histological subtype, it has been demonstrated that Cav-1 enhances tumour growth both *in vitro* and *in vivo* [44,69–71]. Codenotti et al. showed that Cav-1 is able to increase the aggressiveness of ERMS cells (RD) through the cooperation with the Erk-signalling pathway [72]. Erk is a well-known extracellular signal-regulated kinase with a crucial role in many cellular processes including cell cycle progression and survival [73]. They demonstrated that the metastatic RD cells which are characterized by Cav-1 overexpression, also exhibit a marked increase in phosphorylated Erk1/2 (pErk1/2) levels. The involvement of this pathway in the increased cell proliferation in this model has been confirmed by the treatment with PD098059, a synthetic Erk phosphorylation inhibitor: cell proliferation was significantly reduced compared to the untreated cells. The same strategy has been used to demonstrate the correlation between Erk pathway and the increased RD cell migration and invasiveness [72].

Furthermore, Cav-1 is found to be involved in radioresistance in RD cells since its overexpression can enhance ROS neutralization and DNA repair [74]. In order to demonstrate that, RD cells have been treated with a protocol of radiation in fractional doses and those cells overexpressing Cav-1 did not show a significant increase in percentage in G2 phase of the cell cycle (the most sensitive to the radiations) while increased the percentage of cells in S phase (the less sensitive to the radiations), whereas RD-ctrl cells, which do not overexpress Cav-1, behave in the opposite direction. Since it is well known the role of Src kinase in Cav-1 phosphorylation and the role of Akt in post-irradiation cell survival, this result has been confirmed by the treatment with PP2 and LY294002, Src and PI3K inhibitors, respectively [74].

1.3. Extracellular vesicles

Extracellular vesicles (EVs) are lipid bilayer delimited particles naturally released from all the cells to communicate with each other and/or to secrete biological material outside.

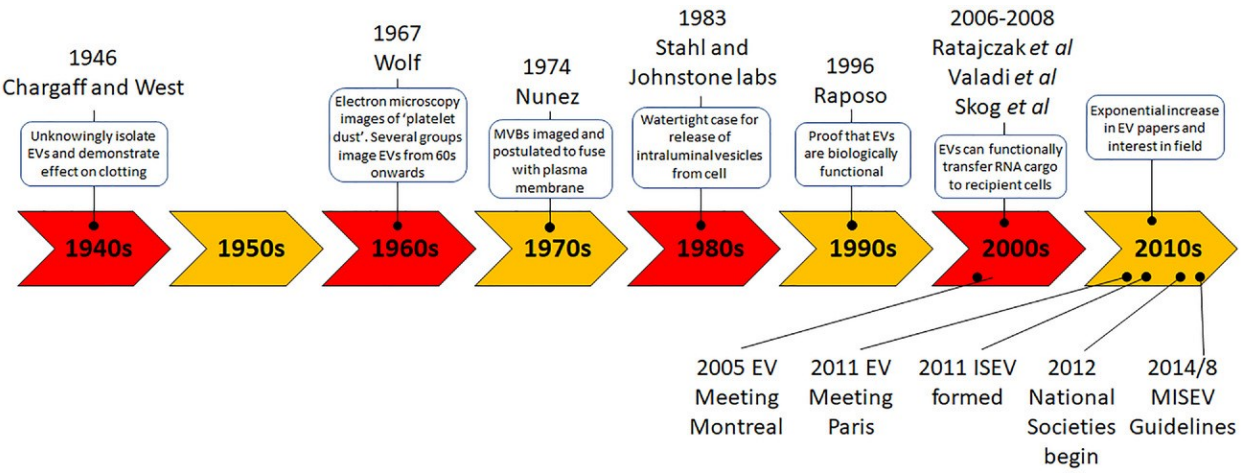

FIGURE 3. The most important steps of EV history**.** (Picture taken from Couch et al., 2021 [75]).

The very first studies were conducted in the 1940s by Chargaff and West in New York. They were a biochemist and a clinician, respectively, studying the blood coagulation and they discovered a “particulate fraction” which sedimented at 31,000 g and with high clotting potential [76]. 17 years later Wolf described a “material in minute particulate form” delivered from platelets, which is sedimented by high-speed centrifugation [77]: we can state nowadays that it was the EV fraction.

EVs were then specifically identified as biological entities, with enzymatic and functional potential, during the 1980s and 1990s. While initially, it was shown that the EV release was a mechanism that cells use to discard unwanted materials, subsequent research demonstrates that it is also an important tool of intercellular communication, involved in both physiological and pathological processes [78–82].

Once released the EVs can be internalized via endocytosis or membrane fusion and release their contents into ‘‘recipient’’ cells [83]. Many studies have shown that these EVs contain various proteins, sugars, lipids, and genetic materials, such as DNA, mRNA, and non-coding (nc)RNAs with the content protected from proteases and nucleases of the extracellular space by the limiting membrane [84,85]. EVs have the ability to deliver combinatorial information to multiple cells in their tissue microenvironment and throughout the body by the blood flow [86–88].

1.3.1. EV classification

EVs can be classified based on their size and biogenesis. Although different scales are used, those with a size range from 50 to 2000 nm are called microvesicles or large EVs (*l*EVs); those with a diameter of 30 to 100 nm are called exosomes or small EVs (*s*EVs); those with a diameter of 500 to 4000 nm are called apoptotic bodies [89]. The overlap in terms of size implies the use of at least another parameter for their identification, like marker expression. Overall EVs comprise a wide variety of vesicles ranging from 30 to 1000 nm in size with a variety of cargos, and the different types of vesicles are similar in their size distribution, so the diameter alone can’t be used as a parameter to define different types of vesicles [90].

In addition to the differences in size, EVs can also be distinguished according to their process of biogenesis: *l*EVs are released outward through budding of the plasma membrane; for the *s*EVs, the release process involves the inward budding of the endosomal membrane, resulting in the formation of multivesicular bodies (MVBs), whose membrane fuses with the plasma membrane releasing the vesicles outside; apoptotic bodies are delivered from dying cells [90].

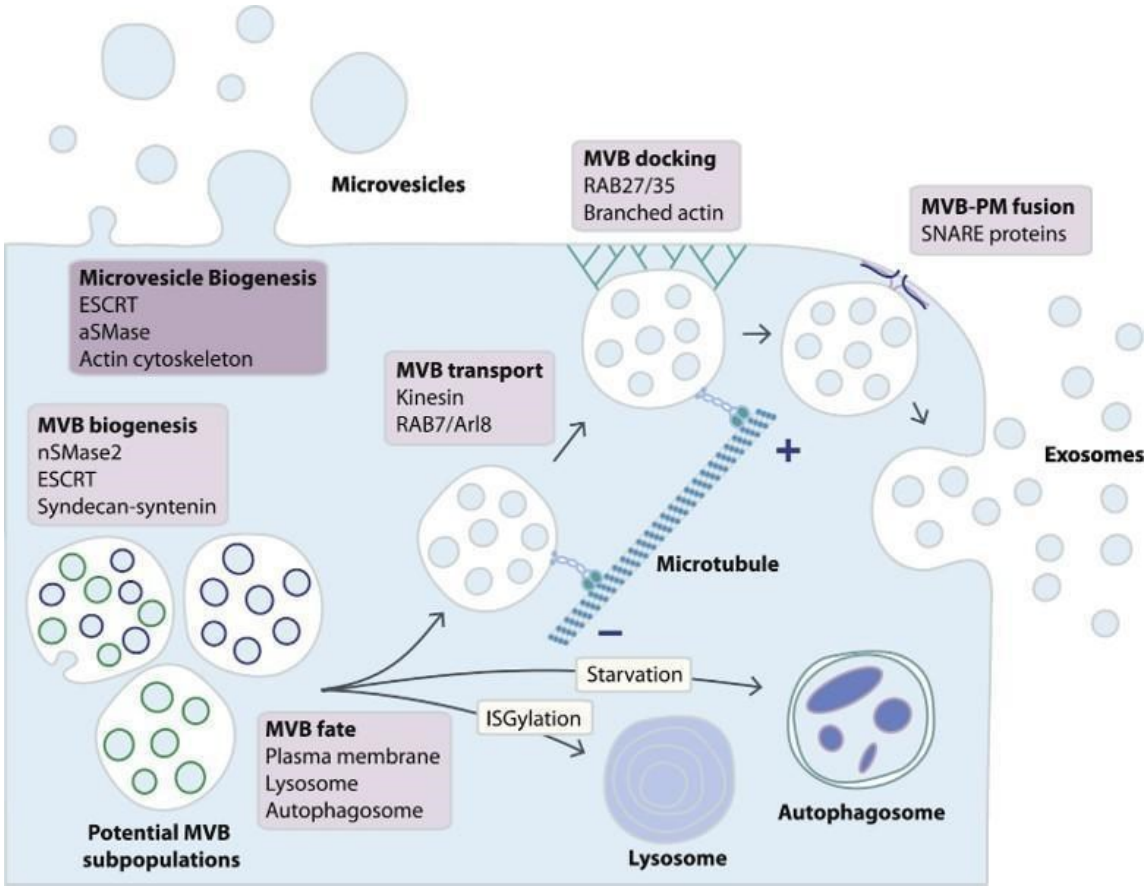

FIGURE 4. Schematic representation of large- and small-EV biogenesis, here called microvesicles and exosomes, respectively. (Picture taken from Babelman et al., 2018 [91])

According to the International Society for Extracellular Vesicles (ISEV 2018 [92]), EVs can be classified according to:

- their physical characteristics, such as size or density
- their biochemical composition

- the descriptions of conditions or cell of origin

In the present work we will focus on the subpopulation of small- and large-EVs and we are going to use the term “small EVs” (*s*EVs) referred to those vesicles that have a <200 nm diameter and are collected with 100K ultracentrifugation, including the ones that originate within MVBs, and the term “large-EVs” (*l*EVs) for those vesicles that have a >200 nm diameter and are collected with 10K ultracentrifugation, including the ones that bud directly from the plasma membrane.

EV SUBSET NAME	SIZE (nm)	BIOGENESIS	BIOMARKERS
large EVs	50-2000	bud directly from the plasma membrane	Calnexin, Grp94
small EVs	30-100	originate within MVBs	Alix, TSG-101, CD9, CD63, CD81
apoptotic bodies	500-4000	originate during apoptosis	caspase-3/7 activity, phosphatidylserine (PS)

Table 1. Classification of EV subpopulations according to their physical characteristics, biogenesis process and typical biomarkers [92].

1.3.1.1 large-EVs

large-EVs are an EV subset with a size range from 50 to 2000 nm and they take origin via direct bud from the phospholipid bilayer. Considering the biogenesis, *l*EV formation is the result of the interplay between cytoskeletal proteins and specific phospholipids: membrane budding is the result of the translocase action to the phosphatidylserine and the subsequent contraction of cytoskeleton by actin-myosin interactions [93–95].

In particular, ADP-ribosylation factor 6 (ARF6) starts a cascade that activates phospholipase D (PLD). In the meanwhile, the Erk recruited to the plasma membrane phosphorylates and activates the myosin light chain kinase (MLCK) which represents the trigger event for the *l*EV release [90]. The external factors that can enhance *l*EV release are the influx of calcium that induces the redistribution of the phospholipids and the hypoxia which has been demonstrated to promote *l*EV release via HIF-dependent expression of RAB22A [96].

1.3.1.2. small-EVs

Small-EVs are 30-100 nm lipid-bound vesicles in which research is mainly focused because of their heterogeneity and biological function.

1.3.1.2.1. *s*EV BIOGENESIS

*s*EV originates through the endosomal pathway. The biogenesis process starts with the endocytosis of the molecular cargo forming a "preliminary" vesicle budding from the plasma membrane inside the cell [97]. This first vesicle formed is called "early endosome" (EE) and its content can undergo three different fates: recycling, maturation for the degradation and maturation for the secretion. When the vesicle cargo needs to be recycled it moves to the EE peripheral tubular domains and it is sorted into the recycling endosomes which can then fuse with the Golgi apparatus or the phospholipid bilayer of the plasma membrane [98]. Recycling endosomal pathway is needed to maintain the correct composition of the plasma membrane since the disruption of this balance is known to be involved in a wide range of diseases including cancer [99]. Among the molecules sorted into recycling endosomes, membrane receptors are the most intuitive to understand, since they should be at the right time to the right place in order to allow or not allow the binding of the ligand [100]. Overall, the "master regulators" of the intracellular vesicular trafficking are the Rab family proteins, among which Rab11 is the main one involved in the recycling process [101].

All the loaded molecules that are not destined to be recycled localize into the central vacuolar region of the EE and go through the maturation of the endosomal pathway. EEs become late endosomes (LEs) or multivesicular bodies (MVBs) which are the final mature endosomal form. MVBs form a number of vesicles by inward invagination of the endosomal limiting membrane (which derives from the initial double invagination of the plasma membrane) resulting in MVBs containing several intraluminal vesicles (ILVs). MVBs can either fuse with lysosomes or with the plasma membrane [102]. This endosomal maturation process implies changes also in the composition of the endosomal membrane, starting from the substitution of sphingomyelin with ceramide and Rab5, a well-established EE marker, with Rab7 which therefore became a good LE marker [98].

The fusion between MVBs and lysosomes occurs whenever the MVB cargo should be degraded. The autophagy process starts with the trapping of the cytoplasmic material within double-membrane vesicles called autophagosomes, which can directly fuse with lysosomes or fuse with MVBs to form amphisomes which will be then degraded together [103]. For this reason, EV release and degradation processes are strictly correlated between each other. It has been demonstrated that the induction of autophagy by starvation reduces *s*EV release [104] whereas the inhibition of autophagy by ATG7 depletion is able to enhance *s*EV secretion [105].

Lastly, when the MVBs fuse with the plasma membrane, ILVs are secreted into the extracellular space and become *s*EVs [98]. The ILV formation step is crucial for the entire process since it determines the future *s*EV composition. One of the most important players in the ILV biogenesis is the Endosomal Sorting Complex Required for Transport (ESCRT) which is a multiprotein complex that coordinates molecular binding and membrane deformation events [98]. Based on this evidence, the main pathway involved in ILV biogenesis is the ESCRT-dependent one, and few ESCRT proteins are also involved in lEV release. The ESCRT pathway is composed of four distinct subsets of complexes called ESCRT 0, I, II, and III which all consist of class E vacuolar protein

sorting (Vps) proteins [106]. All the ESCRT proteins and their functions are summarized in Table 2.

COMPLEX	COMPONENTS	FUNCTION
ESCRT 0	Vps 27/Hrs, Hse1/STAM	binds endosomal limiting membrane and recruits ESCRT I
ESCRT I	Vps 23/TSG101, Vps 28, Vps 37, Mvb12	clusters ubiquitinated proteins under the clathrin coat and recruits ESCRT II
ESCRT II	Vps 22/EAP30, Vps 25/EAP25, Vps 36/EAP45	helps ESCRT and Vps 4 in mediating ILV formation and cargo sorting
ESCRT III	Vps 20/CHMP6, SNF7/CHMP4, Vps 24/CHMP2, Vps 2/CHMP3	mediates membrane remodelling for ILV budding and cargo sorting along with ESCRT II

Table 2. Components and functions of the ESCRT complexes, the main players in *s*EV biogenesis [98].

ESCRT proteins cooperate with other players in ILV generation like ATPase VPS4 (vacuolar sorting protein 4). These components work together sequentially. Initially, ESCRT-0 is recruited to the endosomal limiting membrane, guided by ubiquitin tags on the cytoplasmic domain of transmembrane proteins that are loaded and by PI3P [107]. ESCRT-0 and ESCRT-I then cluster these cargo proteins under a flat clathrin coat, forming an endosomal membrane subdomain that buds into an ILV. This flat clathrin coat prevents cargo protein diffusion and mediates ESCRT-0 dissociation [108]. After that, ESCRT-II and -III are recruited to mediate membrane scission and ILV formation with VPS4 [109]. At the same time, deubiquitinating enzymes are recruited to remove

the ubiquitin tag from cargo proteins before releasing the new ILVs into the lumen of MVBs [110].

Other important pathways for the ILV biogenesis that partially or do not involve ESCRT complexes are:

- Syndecan-Syntenin-ALIX pathway. ALIX interacts with syndecans, a class of transmembrane proteoglycans, through the scaffolding protein syntenin to participate in the membrane budding steps of ILV biogenesis [111].
- Ceramide pathway. Ceramides are membrane sphingolipids enriched in lipid rafts that are able to enhance ILV formation inducing spontaneous negative curvature of the membrane in absence of ESCRT-III [112].
- Tetraspanin pathway. Tetraspanins are a family of small transmembrane proteins that are widely involved in many steps of the *s*EV formation process like cargo sorting [113].

These pathways are therefore considered ESCRT-independent.

It is important to know that proteins involved in the intracellular process of *s*EV biogenesis, then should be found in *s*EV: this is the reason why tetraspanins (CD9, CD81, CD63), ALIX and TSG-101 are considered the main *s*EV markers [114].

During all this biogenesis process, ILV cargo sorting takes place [98]. ILV cargo consists in a variety of different molecules such as proteins, lipids, and nucleic acids which are loaded by different mechanisms. Focusing on protein loading, they are recognized by mono-ubiquitination by ESCRT complexes [115] and right after the loading, ubiquitin is removed thanks to deubiquitinating enzymes recruited by ALIX [116].

Other protein sorting mechanisms that are ESCRT-independent have been discovered: among them, the same mechanism involved in the chaperone mediated autophagy mediated by LAMP2A (lysosomal associated membrane protein 2), has been found to be responsible for the loading of proteins with the KFERQ motif into the ILVs [117].

1.3.1.2.2. *s*EV RELEASE

Once the MVB biogenesis process is complete, mature ILVs that are not driven to degradation pathway, are secreted in the extracellular space becoming *s*EVs. MVBs can fuse with the phospholipid bilayer thanks to vSNARE proteins located on the vesicles, and tSNAREs proteins located on the cell membrane [118]. SNARE proteins, like VAMPs, syntaxins, and SNAPs, are key in fusing endosomal and plasma membranes. VAMP7 on LEs forms complexes with syntaxins to enable this fusion [119,120]. It has been found that VAMP8 assists tau-carrying vesicles in merging with the cell membrane in Alzheimer's models [121]. Syntaxin4 helps Hepatitis C virus to spread by fusing virus-carrying MVBs with infected cell membranes [122]. In Parkinson's models, elevated α-synuclein levels decrease syntaxin4 and VAMP2 interaction, reducing *s*EV secretion [123].

Also, Rab family proteins are involved in this mechanism; in particular, Rab27a and Rab27b actively take part in the vesicular docking at the cell membrane ensuring the correct membrane targeting [124].

1.3.1.2.3. *s*EV UPTAKE BY TARGET CELLS

Once *s*EVs are released into extracellular space they become available for target cells. The exact players involved in EV targeting are not fully understood, and the mechanism whereby *s*EVs have a random or predicted destination remains uncertain [83]. However, *s*EVs can interact with target cells by binding to plasma membrane receptors via *s*EV surface proteins (like tetraspanins, immunoglobulins, and proteoglycans) fusing with the plasma membrane, or undergoing endocytosis (phagocytosis, micropinocytosis, lipid raft-mediated, clathrin-mediated, or caveolin-mediated endocytosis) [125]. In the mechanism of fusion between *s*EVs and the plasma membrane the cargo is released into the cytoplasm of the target cell. Although this is the most efficient delivery way, endocytosis is the predominant uptake mechanism. Once entered, *s*EVs go through the endosomal system and release their cargo into the cytoplasm, trying to avoid degradation, recycling, or direct secretion without affecting

the target cell [80,126,127]. Among the proposed mechanisms for cargo release, there is pH-dependent fusion with endosomes and permeabilization of endolysosomes [128,129]. Since *s*EVs travel in the blood, they must be able to cross the endothelial layer to reach their target. For example, it has been demonstrated that breast cancer-derived *s*EVs enter endothelial cells via clathrin-mediated endocytosis, are sorted by Rab11 for exocytosis at the basolateral membrane and are then secreted through interactions between v-SNARE VAMP-3 on the *s*EVs and t-SNAREs SNAP23 and syntaxin 4 on the cell membrane [130].

1.3.1.3. Apoptotic bodies

Apoptosis is the "physiological" mechanism through which cells die. It's composed of several stages, like nuclear chromatin condensation, membrane blebbing, and the disruption of the cellular content into specific membrane-delimited vesicles called apoptotic bodies or apoptosomes [131]. As apoptotic bodies are released into the extracellular space, they are phagocytes by macrophages thanks to specific receptors that can recognize signal molecules on the apoptotic cell membrane [132]. One of them is Annexin V which is therefore a well-known marker for this EV subset [89].

1.3.2. EVs in cancer

A large body of evidence suggests that EVs are critically involved in the process of tumour growth and dissemination. This is easy to guess since EVs are the main tool for intercellular communication and therefore, over the last decades, the role of cancer-derived EVs within the tumour microenvironment has been extensively researched [91,133].

Many studies have shown that cancer cells release more EVs compared to non-cancer cells, making the EV biogenesis machinery potential target for anticancer therapy. Indeed, overexpression of ESCRT components, syntenin, and heparanase has been

observed in various tumour types [134–139]. Furthermore, cancer-derived EVs have a different protein and RNA cargo compared to normal cell EVs [140–143], which may be the result of oncogenic signalling or altered microenvironmental conditions [144] and which let them exert complex effects on the stromal cells, like endothelial cells and fibroblasts. For example, pancreatic cancer-derived *s*EVs expressing tetraspanin 8 recruit proteins and mRNA that are able to enhance the angiogenesis process in endothelial cells [145]. Moreover, it has been demonstrated that *s*EV containing TGF-β can convert fibroblasts into myofibroblasts, promoting vascularization, tumour growth, and local invasion [146]. Also breast cancer-derived *s*EV can induce the expression of a myofibroblastic phenotype in adipose tissue-derived mesenchymal stem cells, increasing the expression of pro-tumorigenic factors like TGF-β, VEGF, SDF-1, and CCL5 [147]. The same is valid for the tumour stroma-derived *s*EVs: for instance, breast cancer-associated fibroblasts (CAFs) release *s*EVs that can promote tumour motility, invasion, and dissemination through the Wnt signaling pathway [80].

Regarding rhabdomyosarcoma, little is known about RMS-derived EVs. Ghayad et al evaluated the secretome derived from a panel of 5 cell lines (both ARMS and ERMS cell lines). Characterizing the subpopulation of *s*EVs they found that they carry specific miRNA involved in crucial pathways for the cancer signaling networks, like tumour growth, survival, angiogenesis, escape from immune surveillance, migration, and invasion [148]. Another study from Fahs et al demonstrated that the EV derived from human ERMS cell line JR1, and the ARMS cell line Rh41 carry CD147 which contributes to cellular invasiveness and migration abilities [149].

2. AIM

Given the limits in the current knowledge regarding the characterization of RD-derived EVs and their effects, and given the pivotal role of Cav-1 in rhabdomyosarcoma progression, the aim of the present study is to assess whether Cav-1 has an impact on the secretion and loading of RD-derived EVs, and whether EVs could contribute to the increased aggressiveness of RD cells overexpressing CAV-1.

3. MATERIALS AND METHODS

3.1. Cell cultures

For the study we employed three "*in vitro*" model of Human embryonal RD cells (RD-Mock, RD-CAV1^{F0}, RD-CAV1^{F2}) that were kindly provided by Professor Fanzani (University of Brescia, Italy). RD-Mock cells derived from the European Collection of Cell Cultures (ECACC, Salisbury, UK) transfected with an empty vector, RD-CAV1^{F0} are engineered for Cav-1 overexpression [70] and RD-CAV1^{F2} cells derived from the second generation of lung metastases after RD-CAV1^{F0} injection in mice as described in Codenotti et al. [72].

Cells were routinely maintained at 37 °C, 5% CO2 in high-glucose Dulbecco's modified eagle's medium (DMEM) supplemented with 10% heat-inactivated fetal bovine serum (FBS) (Life Technologies, Monza, Italy), 100 mg/ml penicillin/streptomycin (P/S), glutamine 2 mM, 0.5 mg/ml G418 and 1% amphotericin B antibiotics. For all the EV isolation experiments, we used the complete growth medium supplemented with 10% of exo-free FBS. exo-free FBS was obtained by overnight ultracentrifugation at 4 °C and 110,000 g using a SW28 rotor in a Beckman ultracentrifuge, the supernatant was carefully removed with a pipette, passed through a 0.22 µm filter and then added to DMEM.

The human monocytic cell line THP-1 was used as an *in vitro* model of human macrophages and was routinely maintained at 37 °C, 5% CO2 in RPMI medium supplemented with 10% FBS, 100 mg/ml penicillin/streptomycin (P/S), glutamine 2 mM.

3.2. Extracellular vesicle isolation

RD-derived EVs were isolated by using sequential ultracentrifugation methods following the guidelines developed by the International Society for Extracellular

Vesicles (ISEV) in 2018 [92]: cell-conditioned medium was collected and subjected to two serial centrifugations for 30 min at 1000 and 2000 g at 4°C to remove debris and apoptotic bodies. Then, the supernatant was further centrifuged at 18000 g for 30 min at 4°C to obtain large EVs (*l*EVs). The resulting supernatant was further ultracentrifuged at 110,000 g for 2:30 h at 4°C, to obtain small-EVs (*s*EVs).

For proteomic analysis the conditioned medium was collected and ultracentrifuged at 110,000 g for 4 h, to obtain all the EVs. The pellet was then resuspended in sucrose 0,25 M and further separated into 12 fractions by density gradient isolation method. Each fraction was further ultracentrifuged at 50,000 rpm per 2h, The pellets were resuspended in PBS and used for further analyses.

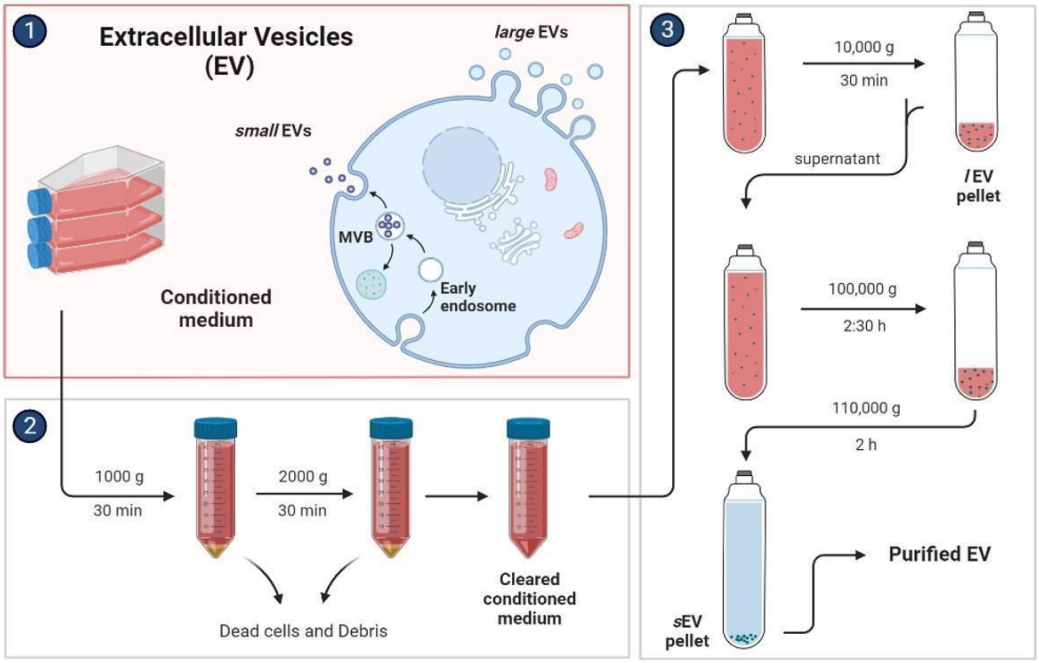

FIGURE 5. Schematic representation of the ultracentrifugation protocol employed in the study to isolate EV subpopulations from RD-cell lines.

3.3. Early (EE) and late (LE) endosome isolation

The separation of EEs and LEs has been conducted at NOVA Medical School, Lisbon, Portugal, during the visiting period at Joao Ferreira's lab according to his instructions

[117,150]. Each RD cell line was cultured in up to two 150 mm plates in its complete medium, then washed and collected with ice-cold PBS and a cell scraper. Cells were pelleted at 300g for 5 min at 4 degrees and resuspended in a homogenization buffer [HB; 250 mM sucrose, 3 mM imidazole (pH 7.4), 1 mM EDTA and 0.03 mM cycloheximide in which they were loosened using cold finger. Samples were then centrifuged at 1300g for 10 min at 4°C and the pellet was gently resuspended with a wide-cut tip in three times the pellet volume of HB. The suspension was passed through a 25-gauge needle, attached to a 1-ml syringe, 10 times. The homogenate was then further diluted in HB (1 part homogenate to 0.7 parts HB) and centrifuged at 1600g for 10 min at 4°C. The supernatant was collected and centrifuged again in the same conditions. The post-nuclear supernatant (PNS) that originated from the second centrifugation contains the endosomal fractions, whereas the pellet contains the nuclei. PNS was then mixed with a 62% sucrose solution (to reach a 40.6% solution) and loaded at the bottom of an ultracentrifuge tube. Excess PNS was used as a separate condition in the downstream WB analysis. The 40.6% solution was overlaid with 1.5 volumes of 35% sucrose solution and 1 volume of 25% sucrose solution, and the tube was filled to the top with HB. The gradient was centrifuged at 210,000g overnight at 4°C, using a 70.1 Ti rotor. LEs are located in the 25%/HB interface whereas EEs are in the 35%/25% one. The endosomal fractions were collected and diluted in 35 ml of HB solution and centrifuged again at 100,000 g for 1 hour in an SW 32 Ti rotor. The organelle pellets were resuspended in PBS and denatured in Laemmli buffer for the WB analysis.

3.3. Nanoparticle tracking analysis

NTA measurements were performed using the NanoSight LM10 (NanoSight, Amesbury, United Kingdom) and three videos of either 30 s or 60 s were recorded of each sample. The NTA 3.1 software (Nanosight) was used for capturing and analysing the data, which are presented as the mean ± SD of the three video recordings. Standards 100 and 400 nm beads were supplied by Malvern Instruments Ltd. (Malvern, UK).

3.4. Western Blot Analysis

Whole proteins were extracted from the organic phase of RD-EVs or cell body samples obtained from QIAzol Reagent lysis (Qiagen User Protocol RY16 May-04). The protein pellet was resuspended in ISOT buffer (8 M urea, 4% CHAPS, 65 mM DTE (1,4-Dithioerythritol), 40 mM Tris base supplemented with SigmaFAST Protease Inhibitor Cocktail (Sigma-Aldrich) and 10 mM Sodium Fluoride. The obtained suspension was sonicated with 10 s pulse and then centrifuged at 12,000 g for 10 minutes at 4 °C.

For cell body samples, protein concentration was assessed by Bradford assay [151] using Bio-Rad Protein Assay Dye Reagent Concentrate (Biorad) and for EV protein by BCA assay. Equal protein quantities were loaded and separated on 10% SDS-PAGE gel and transferred to Immuno blot Polyvinylidene Difluoride membranes, 0.2 µm (PVDF, ThermoFisher Scientific). Primary antibodies used were obtained from commercial sources as follows: LC3B (E7X4S), Grp94 (2104), CD81 (D3N2D), CD9 (D801A), Lamp-1 (D2D11XP) and RAB11 (D4F5) from Cell Signaling Technology; Tsg101 (T5701), Actin (A5060), RAB5 (R4654) and α-tubulin (T5168) from Sigma; Alix (sc-53538) and CAV-1 (sc-894) from Santa Cruz Biotechnology; Syntenin-1 (GTX108470) and RAB7 (GTX132548) from GeneTex; CD63 (TS63) from Invitrogen; Flotillin-1 (ab41927) from AbCam.

For PNS, EE and LE fraction, samples were denatured in Laemmli buffer, and the protein concentration was determined by Micro-BCA assay. The same protein quantity for each sample was separated on a 10% SDS gel and transferred to a nitrocellulose membrane. Primary antibodies used were obtained from commercial sources as follows: EEA1 (SICGEN, AB0006-200); RAB7 (SICGEN AB0033-200); LAMP2A (Abcam, ab18528); LAMP2B (Abcam, ab18529); LAMP2 (SANTACRUZ SC-18822); CD63 (SICGEN AB0047-500); CD81 (SICGEN AB0361-200); HIST3 (Cell Signaling 4499T); FLOT-1 (BD Biosciences 610821).

Primary antibodies were incubated overnight at 4°C, followed by washing and the incubation with specific secondary HRP-conjugated antibodies (Pierce). Immune complexes were visualized using the Clarity and/or Clarity Max Western ECL Substrate

Luminol solution (Bio-Rad). Chemiluminescence was measured using a BioRad ChemiDoc MP Imaging System (BioRad).

3.5. Transmission and Scanning Electron Microscopy

All specimens were fixed in 2% glutaraldehyde/2% paraformaldehyde in 0.1 M phosphate buffer (pH 7.2) overnight at 4°C, then post-fixed in 1% osmium tetroxide for an additional hour. For TEM analysis, fixed samples were dehydrated in an acetone series and embedded in an Epon-Araldite mixture. Thin sections (60 nm) were cut using an MTX ultramicrotome (RMC, Tucson, AZ, USA), stained with lead citrate, and imaged at 80 kV in a Philips CM10 transmission electron microscope (FEI-Thermo Fisher). For SEM, after fixation, samples were dehydrated in an ethyl alcohol series, chemically dried using hexamethyldisilazane (HMDS), mounted on aluminium stubs, coated with gold, and imaged at 10 kV in a Zeiss Supra 40 Scanning Microscope.

3.6. Proteomic analysis

The ProteinGroups file from MaxQuant was initially filtered in Perseus to remove common contaminants, reverse proteins, proteins identified only by site, and those with less than 50% valid values in at least one sample group. After filtering, the matrix was exported to R, performing 5 quantile knn imputation. In groups with more than 50% valid values, the knn algorithm was used; for proteins with less than 50% valid values, missing values were imputed using the sample 5 quantile. The complete, imputed matrix was then re-imported into Perseus, where Welch's T-tests were conducted between the two groups, with the FDR controlled at 0.05 using the Benjamini-Hochberg method.

3.7. Flow cytometry analysis

Flow cytometry analysis has been conducted in order to confirm western blot results on tetraspanins. The same volume of RD-derived *s*EVs was resuspended in dPBS and stained for 30 minutes at room temperature with the corresponding antibodies for surface marker analysis: CD81-PE (BD Biosciences), CD9-FITC (Biotium) and then with ExoBrite™ 640/660 APC - EV Membrane Staining Kit for 30 minutes more at room temperature. Data were analysed using FlowJo software.

3.8. Live-cell imaging

RD-cells were cultured in µ-Slide eight-well chambered coverslips (Ibidi) and treated according to the protocol described by Bright et al, slightly revisited [152]. When cells reached 80% confluence, lysosomes were loaded with SiR-Lysosome which is based on the fluorophore silicon rhodamine (SiR) and the cathepsin D binding peptide pepstatin A. Cells incubated for 2 h at 37°C with SiR-Lysosome in complete growth medium, then we washed with PBS and added Dextran Texas Red for 5 minutes followed by a chase of 5 minutes in conjugate-free medium in order to evaluate the endocytic pathway from the EEs to the lysosomes. Live cells were imaged starting from 5 minutes and up to 40 minutes after the dextran removal, in a Zeiss LSM 710 confocal microscope using a 63x 1.4 Plan-Apochromat oil-immersion objective.

3.9. Lysotracker

Lysotracker staining has been performed to assess any difference in lysosomal activity between the three cell lines. For the fluorescence microscopy analysis, cells were seeded on a glass coverslip in 24-well plate and treated when they reached 80% confluence with Lysotracker Green DND-24 (L7526 Thermo Scientific) 50 nM in complete growth medium: after 2h of incubation at 37°C and 5% CO2 cells were fixed in paraformaldehyde 4% for 20 minutes at room temperature. Nuclear DNA was stained

with 4,6-diamino-2-phenylindole (DAPI, 1:2000 dilution, Sigma). Stained samples were mounted in Mowiol 4-88 (Sigma-Aldrich) and photographed using a DC300F digital camera connected to a Fluorescence microscope (IM50 software Leica, Wetzlar, Germany). For the flow cytometry analysis cells were seeded in a 6-well plate and after 2h of incubation with Lysotracker at the same concentration and conditions as above, cells were trypsinized, collected in PBS and analysed with FACSMelody Cell Sorter. The acquired data were analysed by ImageJ and FlowJo softwares, respectively.

3.10. Wound healing assay

Huvec cells were seeded in 6-well plates and pre-treated for 2 h with 10 μM PD098059 or DMSO; as they formed confluent monolayers they were wounded by scraping the cells with a 200 μl-sterile micropipette tip. Images of wound healing were acquired after 0 h, 3 h and 6 h by an inverted light microscope (Olympus IX50; Olympus, Tokyo, Japan) using CellR Software (Olympus, Tokyo, Japan). The percentage of wound repair was quantified by measuring the healed area using ImageJ software. Results were presented as a percentage of the repaired area respect to time 0 h (CTRL).

3.11. Transwell migration assay

Migration Assay was performed by using Transwell permeable supports with a membrane lterof 8 μm pores: HUVEC cells were seeded on the top of the membrane and treated for 24 h with purified *s*EV (2,5 – 5 – 10 μg/ml) and with the supernatants (collected after sEV centrifugation) concentrated with 10 kDa membrane to obtain concentrated total proteins (25 – 50 – 100 μg/ml).

3.13. Statistical analysis

Analyses were conducted by using unpaired Student's t test and One-Way Anova test, GraphPad Prism 8 software (GraphPad Software, San Diego, USA). Statistical analysis

was performed using Student's t-test, one-way ANOVA with either a Tukey's (parametric) or Kruskal-Wallis (non-parametric) post hoc test unless otherwise stated. Statements of significance were based on a p-value of less than 0.05. Significance is equal to *$p < 0.05$, **$p < 0.01$, ***$p < 0.001$ and ***$p < 0.0001$.

4. RESULTS

4.1. Extracellular vesicle secretion increases in caveolin-1 overexpressing cells

Despite the controversial role of Cav-1 in cancer progression, recent studies have demonstrated that Cav-1 overexpression increases metastasis formation in a human model of embryonal rhabdomyosarcoma (RD) [72]. Furthermore, it has been shown that Cav-1 has not only a structural role in the plasma membrane but can also affect the EV release [24].

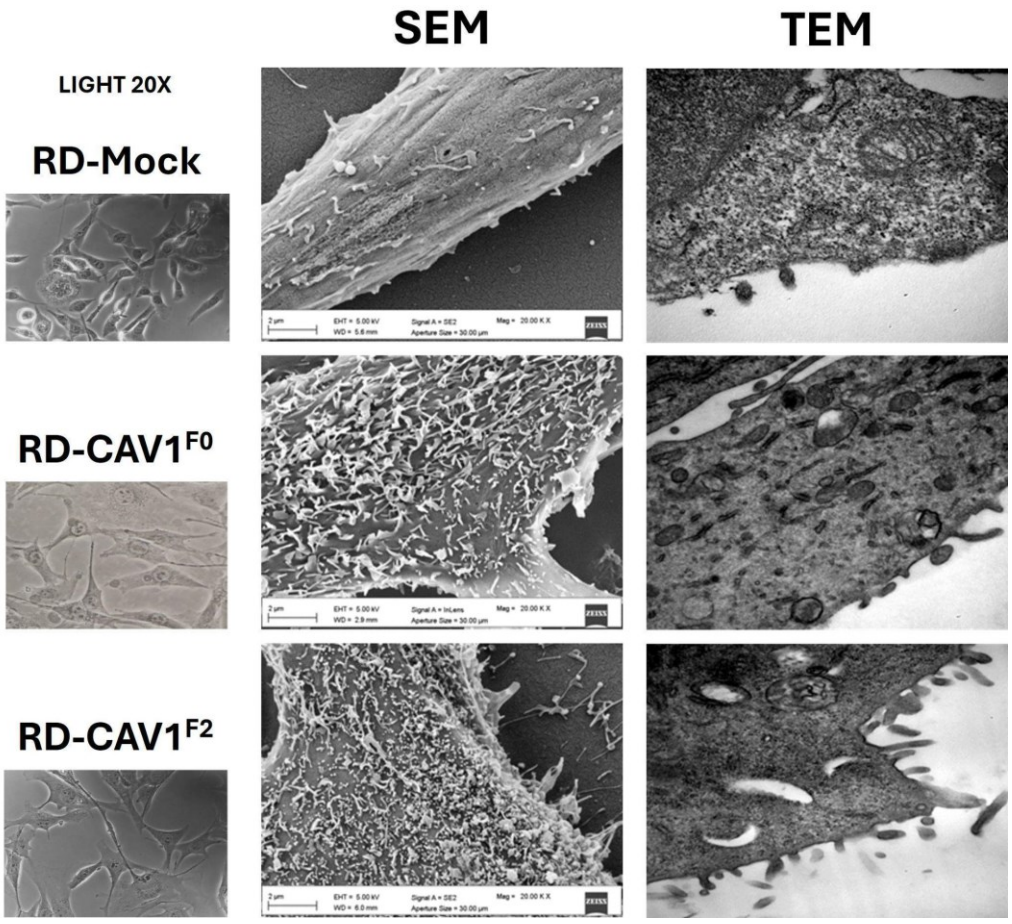

FIGURE 6. Morphological analysis of RD-cells through scanning and transmission electron microscopy techniques (SEM and TEM) highlighted the higher number of protrusions and MVB-like formations in RD cells overexpressing Cav-1 compared to the control.

Given the potential role of EV in the enhancement of tumour progression and in order to assess whether Cav-1 overexpression correlates with an altered EV release in rhabdomyosarcoma, we employed three RD cell lines: RD-Mock, which does not overexpress Cav-1, and RD-CAV1^{F0} engineered for Cav-1 overexpression, and RD-CAV1^{F2} derived from the second generation of lung metastases after RD-CAV1^{F0} injection in mice, which have already been proven to be characterized by higher cell proliferation, migration and invasiveness [70, 72]. We first performed scanning and transmission electron microscopy analyses (Fig. 6), and we saw a greater number of protrusions in RD cell overexpressing Cav-1 compared to RD-Mock, which means that these cells undergo to a deep plasma membrane reorganization that may correlates with a higher EV release.

Furthermore, TEM analysis revealed a higher number of intracellular organelles surrounded by membranes that look like MVBs in RD cells overexpressing Cav-1 compared to RD-Mock. We then assumed that this morphological information could correlate with the hypothesis that Cav-1 overexpression may be able to increase RD-EV production.

According to the Minimal Information for Studies of Extracellular Vesicles guidelines by the International Society for Extracellular Vesicles (MISEV 2018) [92] in which Nanoparticle Tracking Analysis (NTA) is one of the first steps for the proper EV characterization, we performed it to further confirmed our hypothesis. The three cell lines were incubated in their complete medium with exosome free-FBS for at least 72 h; the conditioned media were then collected and processed by a protocol of sequential ultracentrifugation according to the guidelines [92].

NTA revealed the correct size of the two EV subpopulations obtained (Fig. 7A) and highlighted that RD cells overexpressing Cav-1 release 3-4 fold more EVs compared to RD-Mock, as expected. In particular, RD-CAV1^{F0}- and RD-CAV1^{F2}-derived *s*EV are found to be 10 times more abundant than *l*EVs released from the same cells (Fig. 7B), making us more interested in the subpopulation of *s*EVs for the subsequent analyses.

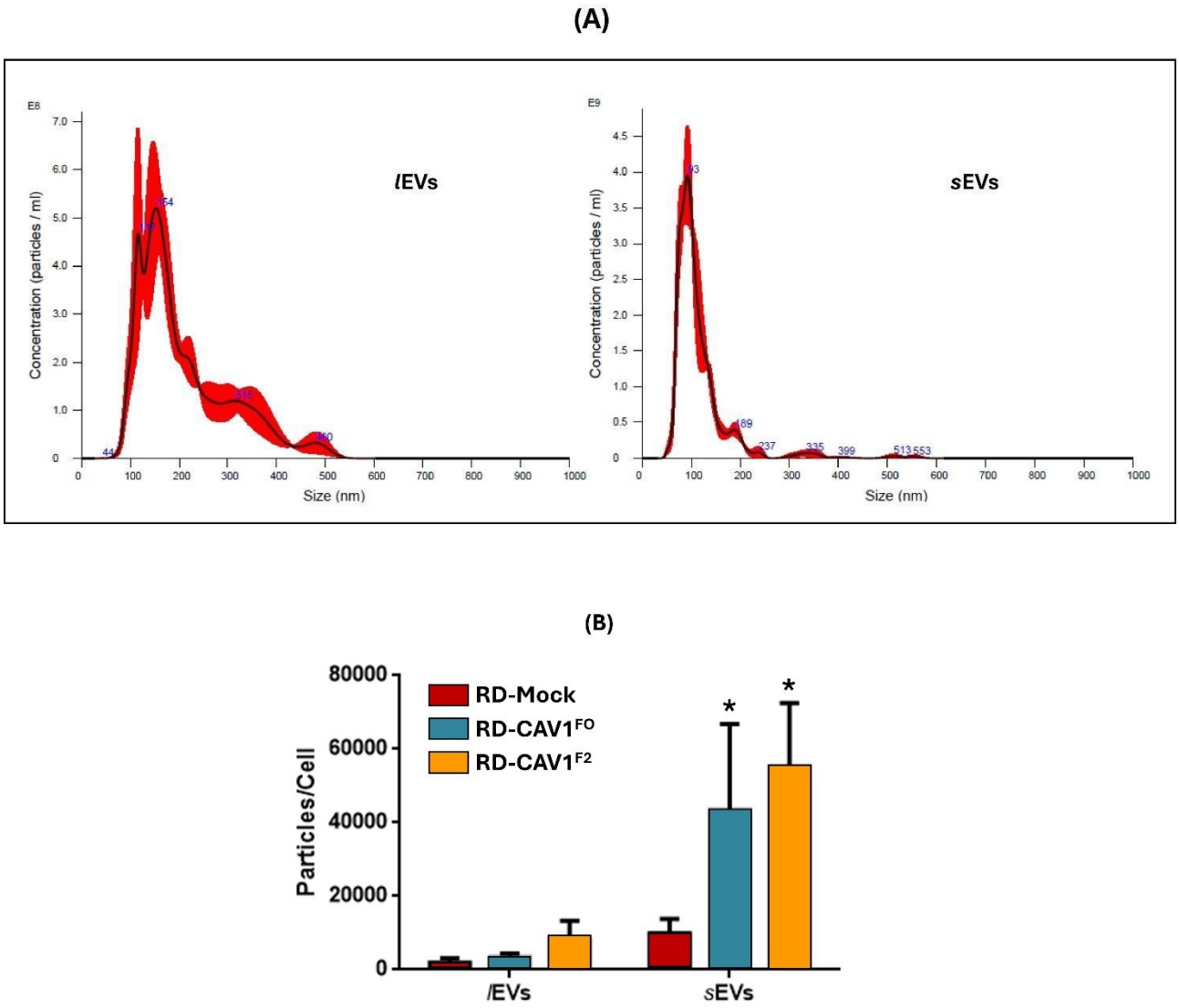

FIGURE 7. (A) Nanoparticle Tracking Analysis (NTA) confirmed the correct size of the isolated *l*EVs and *s*EVs and (B) demonstrated that RD-CAV1^{F0} and RD-CAV1^{F2} cells release a higher amount of vesicles, particularly *s*EVs, compared to RD-mock.

Overall, morphological analysis and NTA analysis demonstrated that Cav-1 overexpression is correlated with an increased vesiculation which could be one of the factors contributing to the acquired aggressive metastatic behaviour of the RD-CAV1^{F0} and RD-CAV1^{F2} cells.

4.2. Caveolin-1 overexpression induces the release of tetraspanin-free *s*EVs.

Right after the physical characterization, we moved on with the analysis of the key EV markers by western blot analysis (WB) in which we demonstrated the presence of Alix, Flotillin-1, Syntenin-1, and TSG101 in the *s*EV subpopulation, and of the endoplasmic reticulum marker Grp94 in the *l*EV one (Fig.8A).

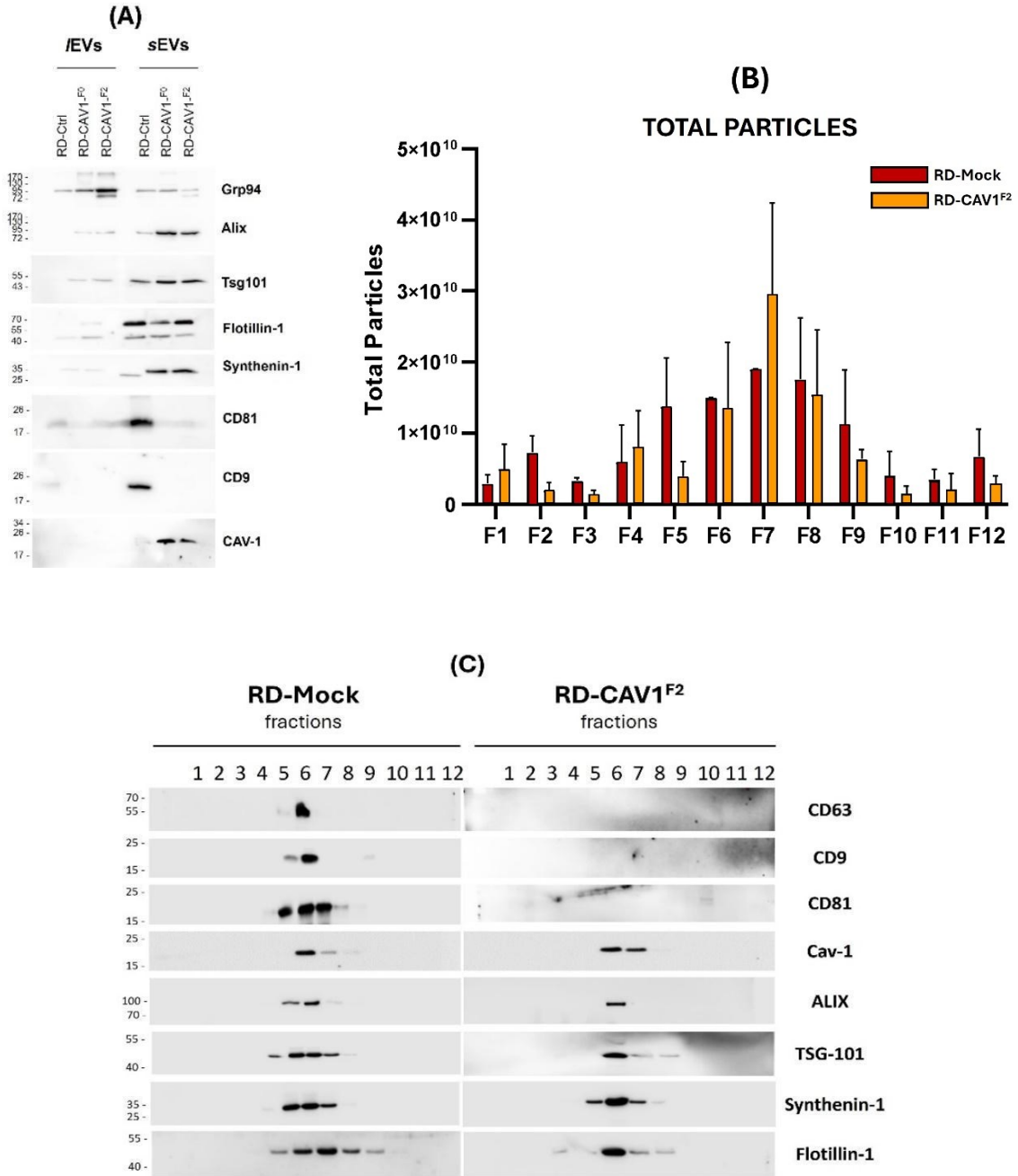

FIGURE 8. (A) Western blot analysis confirms the presence of typical markers in both EV subpopulations, except for CD9 and CD81 which are not detected in RD-CAV1-derived *s*EVs. Density gradient separation was performed to further purify *s*EV samples: (B) among the 12 fractions obtained, 6 and 7 were found to be the most enriched ones in 80-120 nm particles. (C) Western blot analysis performed on all the RD-Mock and RD-CAV1^{F2}- derived fractions confirmed previous data about the expression of Cav-1, Alix, TSG-101, syntenin-1 and flotillin-1, without detecting CD81, CD9 and also CD63 in RD-CAV1-derived *s*EVs.

Cav-1 levels have been confirmed to be higher in RD-CAV1^{F0} and RD-CAV1^{F2} derived EVs, as expected, while we surprisingly detected CD9 and CD81 only in RD-Mock derived EVs (Fig.8A). This finding opened a consideration about the potential ability of Cav-1 to alter the *s*EV protein composition together with the amount of their secretion. In order to confirm these data, we further purified the *s*EV subpopulation by Optiprep density gradient separation and we found that fractions 6-7 were the most enriched fractions in 80-120 nm particles (Fig. 8B). Moreover, WB analysis performed on all the fractions confirmed the presence of the typical biogenesis markers like TSG-101 and Alix and their enrichment in the same fractions revealed by NTA (Fig. 8C). WB analysis also confirmed the expression of CD81 and CD9 only in RD-Mock derived fractions and extended this data to CD63, which has been also undetected in RD-CAV1^{F0} and RD-CAV1^{F2} derived fractions (Fig. 8C).

Given the well-known relevance of tetraspanins, and in particular of CD63, in the whole extracellular vesicle machinery function [153], we further investigate this atypical tetraspanin expression on the whole cell bodies from all the three cell lines. As shown in Fig. 9A, CD9, CD63 and CD81 are not detected in RD-CAV1^{F0} and RD-CAV1^{F2} whole cell lysate and the same result has been obtained by flow cytometry analysis (Fig. 9B upper panel) in which RD-CAV1^{F0} and RD-CAV1^{F2} histograms always overlap, and the more positive one is the RD-Mock sample for all the three tetraspanins. An equivalent outcome has been obtained by the flow cytometry analysis of the *s*EV subpopulation (Fig. 9B lower panel). One of the challenges to analyse vesicles with flow cytometers is related to their dimension, and the main risk is to take into account the background

particles during the sample processing. In order to avoid this problem, we first stained *s*EVs with ExoBrite™ 640/660 APC which is a specific EV Membrane Staining Kit used to be sure that the ones analysed downstream were effectively lipid-bound vesicles, prior to the staining with the tetraspanin antibodies.

Once we assessed the lower expression of the tetraspanin proteins both in the *s*EVs and in the CBs of the RD-CAV1^{F0} and RD-CAV1^{F2} samples, we decided to determine their mRNA expression levels and surprisingly, we didn't find significant differences among the three cell lines (Fig. 9C).

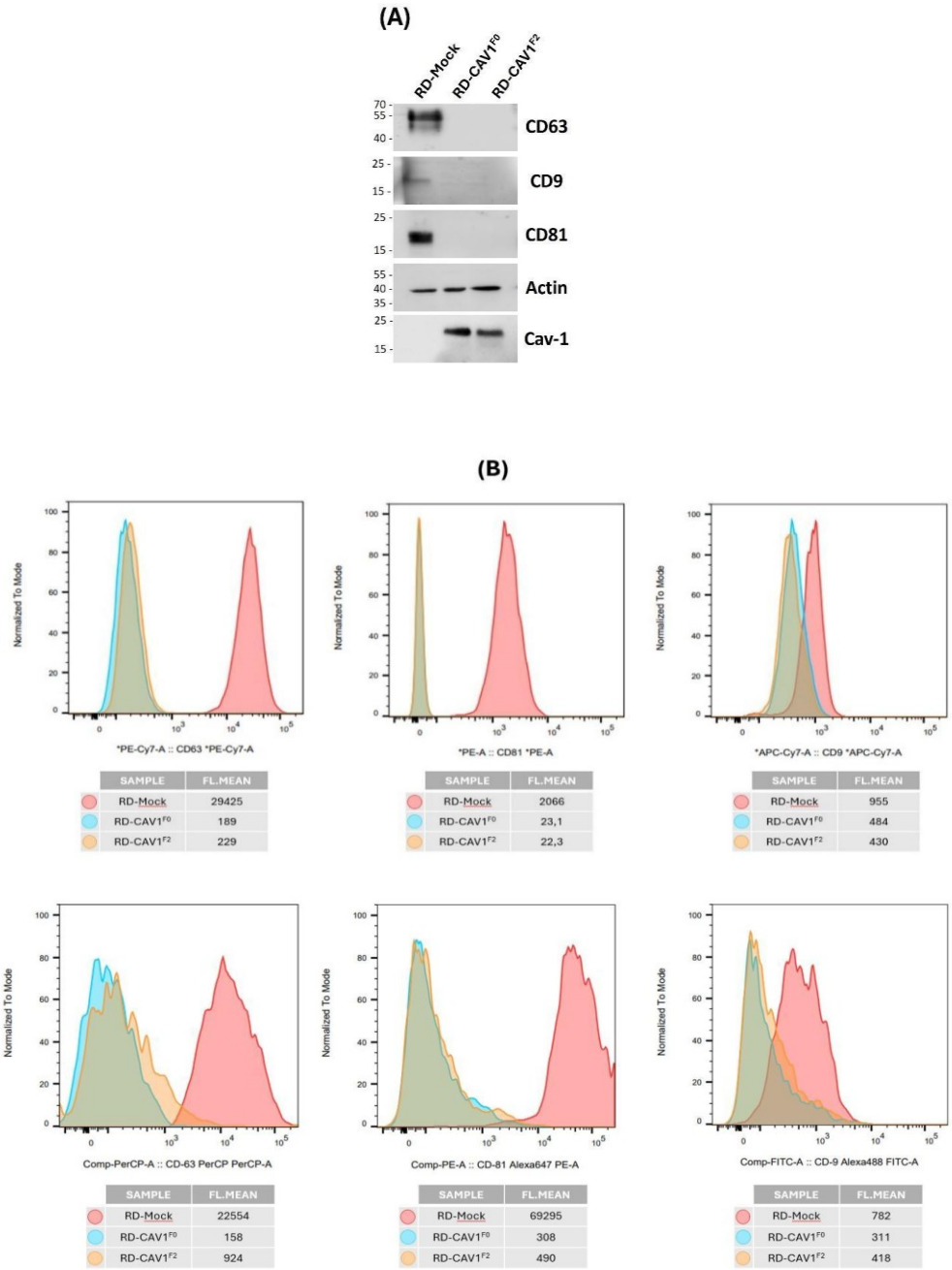

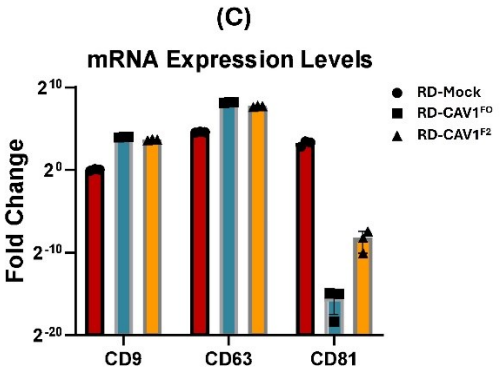

FIGURE 9. (A) In the western blot analysis performed on the whole cell extracts of the three cell lines CD81, CD9 and CD63 tetraspanins are not detected in RD-CAV1 samples. (B) Flow cytometry analysis was performed on both cell bodies (upper panel) and *s*EV subpopulation (lower panel) and confirmed the decreased levels of each tetraspanin in RD-CAV1 samples. (C) CD9, CD81 and CD63 mRNA expression levels are almost unchanged among the three cell lines, suggesting that post-transcriptional factors may be involved in this mechanism, instead of gene loss.

This result corroborates with flow cytometry data in which we do not assist to a lack of tetraspanins in RD samples overexpressing Cav-1, but to a decrease of their expression compared to the control, suggesting that other factors (such as miRNA) may be involved in this mechanism, instead of the gene loss.

4.3. *s*EV protein profile is altered in caveolin-1 overexpressing cells

It has already been demonstrated that tetraspanin expression can undergo up- or downregulation for several reasons in cells, and subsequently in *s*EV. In order to further understand this mechanism in our model and to acquire more information about Cav-1's impact on the overall *s*EV protein loading, we performed the proteomic analysis. *s*EV subpopulations derived from RD-Mock and RD-CAV1^{F2} cells were further purified by Optiprep density gradient separation as previously described, and the extracted proteins from the most enriched fractions were subjected to LC–MS/MS proteomic analysis. The comparison between our *s*EV proteomic data and the EV database

Vesiclepedia [154] showed that most of the proteins found in our datasets have been previously identified in other EV studies, confirming the strength of our purification protocol.

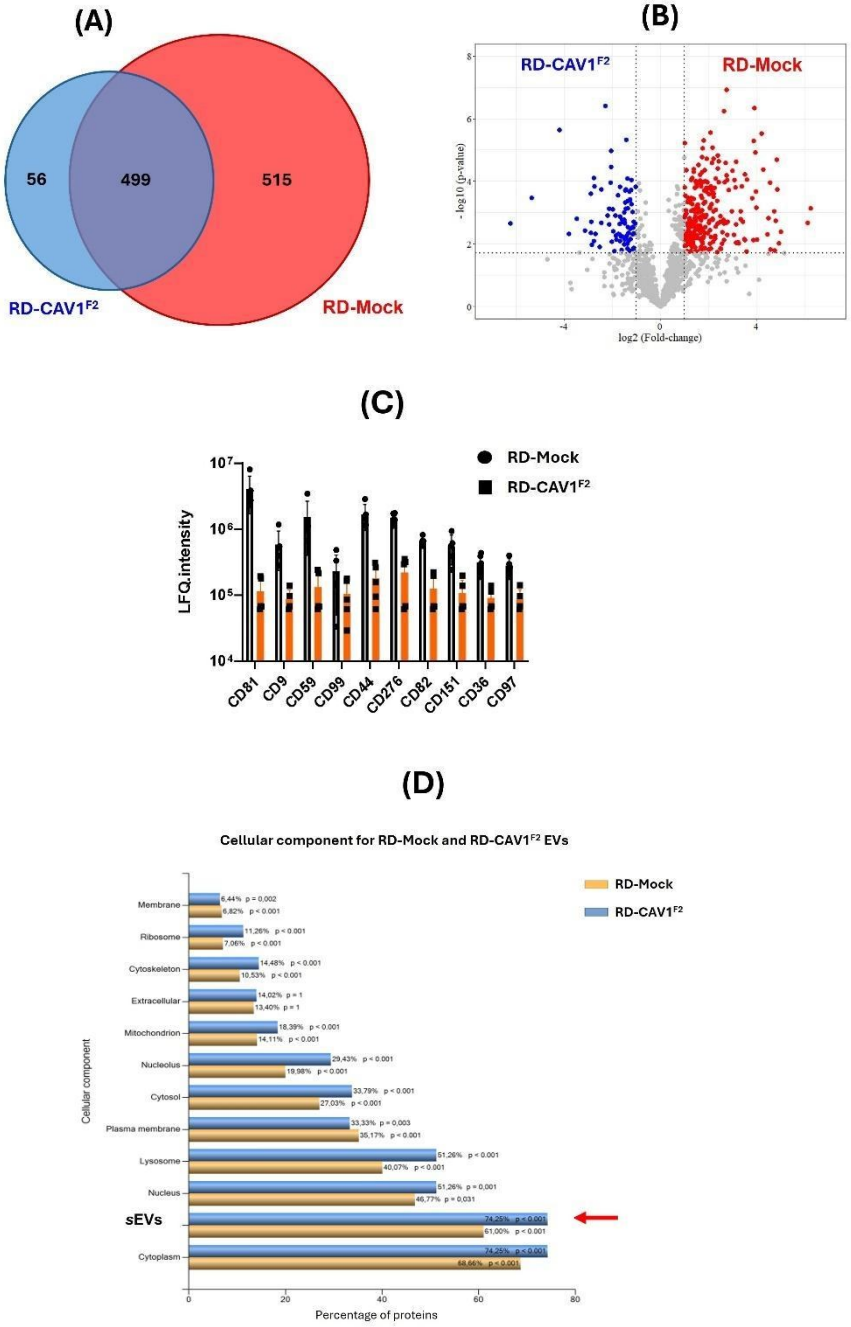

FIGURE 10. Proteomic analysis was performed on RD-Mock- and RD-CAV1^{F2}- derived *s*EV subpopulation, previously purified by density gradient separation. (A) Less amount of protein has been detected in RD-CAV1^{F2} samples compared to the control. (B) The volcano plot confirmed that RD-CAV1^{F2} *s*EVs are characterized by an overall less protein cargo and demonstrated that these proteins are also less expressed. (C) Proteomic analysis also confirmed western blot and flow cytometry findings on CD expression and extended these

results to many other tetraspanins. (D) The distribution of the identified proteins within the various cellular components shows that a high percentage of them are typical of the *s*EV subpopulation.

As shown in Fig. 10A, we found around 1000 different proteins expressed in RD-Mock-derived *s*EVs and only 555 in RD-CAV1^{F2}-derived *s*EVs with 499 shared proteins. The volcano plot (Fig. 10B) highlights that RD-CAV1^{F2} derived *s*EVs not only have a lower protein load compared to the control but also that those proteins are less expressed. Indeed, focusing on tetraspanins, it has been confirmed that CD9 and CD81 expression is lower in RD-CAV1^{F2} derived *s*EVs compared to the control, and this data has been extended to many other CDs (Fig. 10C). Moreover, proteomic analysis revealed the distribution of the identified proteins within the various cellular components and a high percentage of them are found to be typical of the *s*EV subpopulation, validating both the integrity of the *s*EV isolation method employed and their biogenesis from MVBs (Fig.10D).

Overall, with the proteomic analysis we confirmed the WB and flow cytometry results regarding the tetraspanin expression, and we demonstrated that Cav-1 overexpression has an impact on the whole *s*EV protein loading, since RD cells overexpressing Cav-1 release more but “emptier” vesicles compared to RD-Mock.

4.4. Caveolin-1 overexpression enhances intracellular vesicular trafficking

Given the huge differences that Cav-1 overexpression is found to induce in the amount of EV secreted as well as in their protein loading, the next step was to further understand if there were such extensive changes also in the intracellular vesicular trafficking, from which *s*EV biogenesis and secretion are closely dependent.

As previously anticipated, Rab proteins are a family of small GTPases with a key role in the process of intracellular vesicular trafficking [155]. It is well-known that Rab5, Rab7 and Rab11 are the key endosomal Rabs involved in the EE: Rab5 has multiple functions in the EEs interacting with a number of downstream target like class C core vacuole/endosome tethering (CORVET) complex or EEA1 [156] and more recent studies

found that it is involved in the recruitment and activation of ESCRT II [157]; Rab7 is the most important component of LEs since it actively participates in their biogenesis and fusion [158]; Rab11 is mainly involved in the endosomal recycling machinery [101]. Fig. 11A shows that the expression of Rab5, Rab7 and Rab11 is higher in the protein extract of RD-CAV1^{F0} and RD-CAV1^{F2} cell bodies compared to the RD-Mock sample. The same happens to Flotillin-1, a protein enriched in lipid rafts, which is a key player in the endocytic pathway (Fig. 11A). Another important endosomal marker is the lysobisphosphatidic acid (LBPA), an atypical phospholipid which is found to be enriched in LEs and in ILVs [159]. Our immunostaining results (Fig. 11B higher panel) show a progressive increase in the presence of LBPA from RD-Mock to RD-CAV1^{F2} cells, confirming the relative higher abundance of mature endosomes where Cav-1 is overexpressed. The same result was obtained with the syntenin-1 immunostaining (Fig. 11B lower panel). Syntenin-1 is an ubiquitous protein with several intracellular functions [160] which is recently found to be involved in ILVs biogenesis by interacting with syndecan and ALIX in an ESCRT-independent manner [111]. In our model, higher Syntenin-1 expression in RD cells overexpressing Cav-1 (Fig. 11B lower panel) corroborates with all the previous data about Rabs, flotillin-1 and LBPA, indicating that Cav-1 can induce deep modifications in the intracellular secretory machinery.

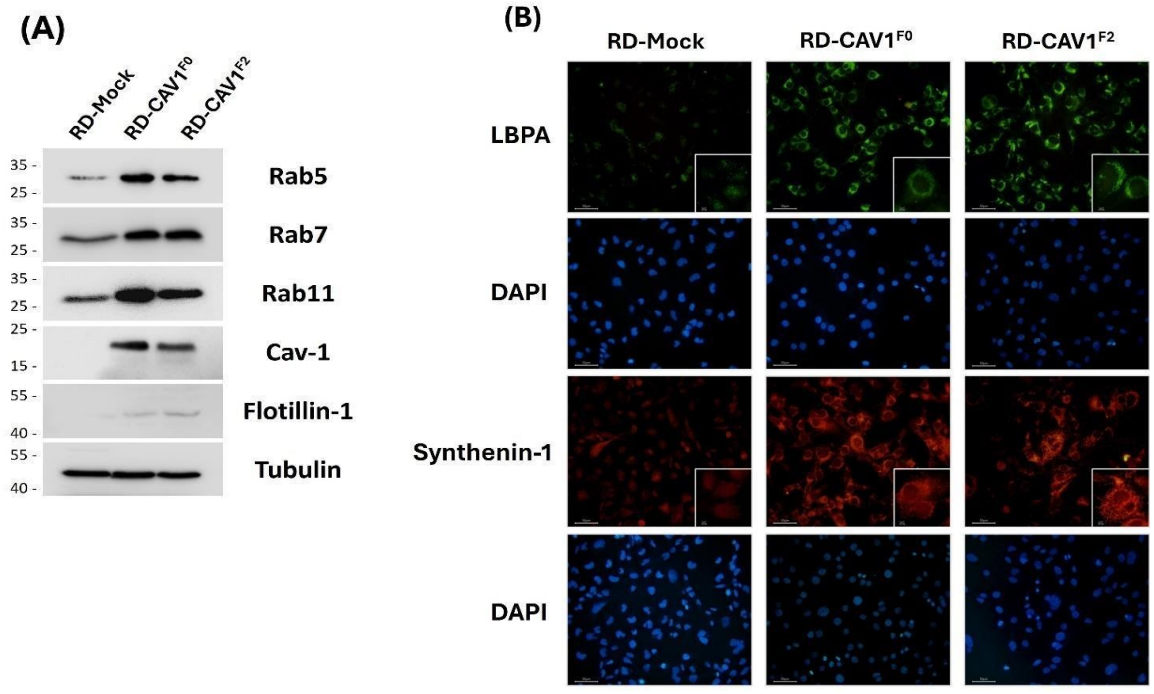

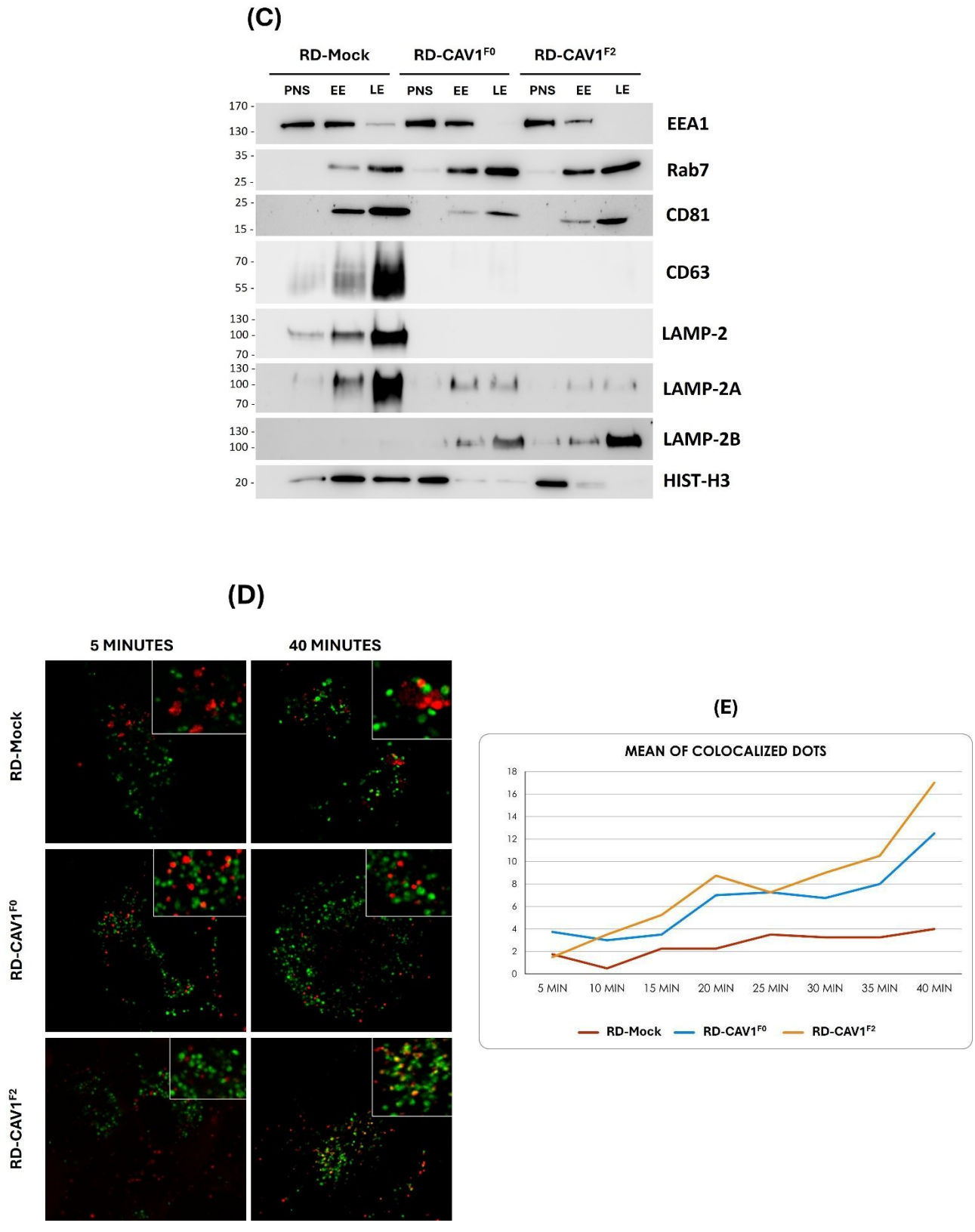

FIGURE 11. Cav-1 overexpression induces an increase in intracellular vesicular trafficking. (A) Western blot analysis shows higher expression of flotillin-1 and Rab proteins in RD-cells overexpressing Cav-1 compared to the control. (B) LBPA and syntenin-1 were found to be more represented in RD-cells overexpressing Cav-1 by immunostaining. (C) Endosomal fraction

isolation confirms CD63 and CD81 data and demonstrates LAMP2A decrease in RD-CAV1 samples, providing a possible explanation for the lower vesicular load in RD-CAV1-derived *s*EVs. (D, E) Live cell imaging demonstrates the higher speed of dextran endocytosis in RD-cells overexpressing Cav-1 showing a higher number of colocalized dots at each time point compared to RD-Mock.

In order to further investigate the expression trend of the key endosomal markers we performed the isolation of the EE and LE endosomal compartments from the three RD cell lines (Fig. 11C). Following the detailed protocol previously described (Section 3.3), we obtained three samples for each cell line: post-nuclear supernatant (PNS), EEs and LEs which were then subjected to the western blot analysis. EEA1 and Rab7 expression levels confirmed the correct isolation with non-significant contamination among the EE and LE fractions. Interestingly, Rab7 follows the same trend of expression found in the whole cell bodies through the endosomal pathways of the three cell lines, with a 5-fold increase in RD-CAV1^{F2} derived LEs compared to the control. Therefore, the higher (although not that relevant) expression levels of EEA1 in RD-Mock derived EEs may be explained by the lower rate of endosomal maturation compared to RD cells overexpressing Cav-1. The flotillin-1 expression trend on the PNS fractions confirms the WB data on the cell bodies (Fig.9A) while its expression in endosomal compartments is overall higher in RD cells overexpressing Cav-1, supporting the WB data obtained from the *s*EV fractions (Fig.8A, C). The same is true for CD81 expression levels which are lower in RD-CAV1^{F0} and RD-CAV1^{F2} derived LEs compared to the control; even more noticeable are the different expression levels of CD63 which has been detected only in RD-Mock fractions (Fig. 11C). All these endosome-related data not only give feedback of the key marker expression levels and their differences among the three cell lines, but also it also provides the evidence that those isolated and analysed, despite the downregulation of certain typical markers (e.g. tetraspanins CD9, CD81 and CD63), are effectively *s*EVs originating from the endosomal pathway.

Furthermore, given the recent findings on LAMP2A about its involvement in the loading of specific protein subset containing KFERQ motif into the *s*EVs [117] and given the deep differences in the protein cargo in our model, we decided to further evaluate its

expression into the endosomal compartments and we found that it's less detected in RD-CAV1^{F0} and RD-CAV1^{F2} derived LEs compared to the control (Fig. 11C). In order to confirm this data we also checked for the expression of HIST-H3 (histone-H3), a nuclear protein which contains the KFERQ motif. WB revealed its presence in all the RD-derived PNS fractions but its loading in the endosomal machinery was detected only in RD-Mock samples. This finding is in line with the evidence of the proteomic analysis in which we found an overall less protein loading in RD-CAV1^{F0} and RD-CAV1^{F2} derived *s*EVs, and this could be one of the mechanisms involved in it. Notably, the isoform LAMP2B exhibits an opposite trend compared to LAMP2A, significantly increasing as a compensatory mechanism, while total LAMP2 is undetectable in RD-CAV1^{F0} and RD-CAV1^{F2} samples. This result suggests that Cav-1 overexpression might induce post-translational modifications to LAMP2 isoforms in the shared epitope recognized by the total LAMP2 antibody, making them detectable only in RD-Mock samples; this is a preliminary hypothesis that needs further insights.

Lastly, starting from the evidence of the increased intracellular vesicular trafficking, the higher maturation of the late endosomal compartments and the increased vesicle released in Cav-1 overexpressing cells compared to the control, we further investigated upstream in the process focusing on the endocytosis mechanism. RD-Mock, RD-CAV1^{F0} and RD-CAV1^{F2} cells were incubated with SiR-Lysosome and Dextran Texas Red according to the protocol previously described (section 3.8). Since Sir-Lysosome localizes in the lysosomal compartments binding cathepsin-D and dextran is a high molecular weight polysaccharide that has generally been used as a marker for macropinocytosis [117,161], we performed live cell imaging in order to evaluate any differences in the endocytic pathway from the EEs to the lysosomes among the three RD-cell lines. Images were taken with a confocal microscope starting from 5 and up to 40 minutes after the dextran removal. Here we show the first and the last sets of images of the three cell lines (Fig. 11D). SiR-Lysosome (green dots) correctly labelled the RD-Lysosomes and dextran (red dots) properly entered inside the cells. The first set of images shows poor colocalization in all the three cell lines whereas at 40 minutes after

the dextran removal is evident the higher amount of colocalized dots in RD-CAV1^{F2} cells compared to the RD-Mock ones. By counting the number of colocalized dots at each time point by ImageJ software and considering the average of 4 pictures taken at each time-point for both the cell lines, we can conclude that dextran goes faster through the endocytic pathway in RD cells overexpressing Cav-1 (Fig. 11E), confirming that Cav-1 overexpression induces intracellular modifications leading to an increased vesicular trafficking.

4.5. Lysosomal function is impaired in caveolin-1 overexpressing cells

Given the effects of Cav-1 overexpression on endosomal trafficking and given the close connection between endosomes and lysosomes, another relevant aspect that we have explored is related to the lysosomal functions. As previously mentioned, MVBs can either be directed to lysosomes for degradation or transported to the plasma membrane for EV secretion [103]. Recently, it has been demonstrated that Cav-1 overexpression can induce ROS production, which potentially leads to lysosomal disruption [162]. The subsequent lysosomal dysfunction might shift multivesicular bodies from degradation pathways to plasma membrane fusion, leading to an increased EV secretion in cells overexpressing Cav-1. In order to test this hypothesis we first checked for the presence of the main lysosomal proteins such as the lysosomal-associated membrane proteins 1 (LAMP1) and 2 (LAMP2). WB analysis performed on the RD-cell bodies did not detect LAMP1 in RD cells overexpressing Cav-1 (Fig. 12A) corroborating with the LAMP1 immunostaining analysis (Fig.12B). The same result has been obtained for LAMP2 (Fig. 12A), confirming the outcomes from the endosomal compartment analysis. We also looked for the presence of Cathepsin-B, a lysosomal cysteine peptidase which, conversely, was found to be more represented in RD-CAV1^{F0} and RD-CAV1^{F2} cells compared to the control (Fig. 12A). Furthermore, Lysotracker Green DND-24 has been used to assess any differences in the acidity (e. g. activity) of the lysosomal compartments. Both immunostaining and flow cytometry analyses

highlighted the fluorescence decrease in RD-CAV1^{F0} and RD-CAV1^{F2} cells (Fig. 12C), demonstrating less activity of Cav-1 overexpressing cell lysosomes. Given the Lysotracker outcome and since Cathepsin-B works only at low pH [163], we also performed a preliminary functional assay in order to evaluate its activity instead of just the protein expression levels. Magic Red Cathepsin B kit (Biorad) was used to stain RD- cells according to the manufacturer's instructions for adherent cells. Cells were then detached and fixed in suspension in paraformaldehyde 4%, washed and analysed by flow cytometry. The histogram shows a progressive decrease of the protease activity in RD cells overexpressing Cav-1 compared to the control (Fig.12D). We can conclude that in RD-CAV1^{F0} and RD-CAV1^{F2} cells Cathepsin B, as well as Cathepsin-D previously identified by SiR-Lysosome staining, is expressed but its activity is lower compared to RD-Mock cells, confirming the Lysotracker data about the decreased lysosomal acidity. Moreover, in these cells the mRNA expression levels of many players in the autophagy machinery like ATG, LC3, NBR1, ULK1, WDR45, p62 and beclin, were found to be lower compared to the control (Fig. 12E). LC3 (autophagy marker Light Chain 3) undergoes cleavage at the carboxy terminus immediately after synthesis, resulting in the cytosolic form LC3-I which, during autophagy, is lipidated by a ubiquitin-like system involving Atg7 and Atg3, converting it into LC3-II. The presence of LC3 in autophagosomes and the conversion of LC3-I to the lower migrating form LC3-II, are widely used as markers of autophagy [164–167]. Therefore RD-Mock and RD-CAV1^{F2} cells were subjected to starvation by FBS deprivation and collected after 1h - 4h - 24h. WB analysis performed on the cell bodies demonstrated the lower LC3-I / LC3-II conversion in RD-CAV1^{F2} cells at each time-point, confirming the less autophagic activity compared to the control (Fig. 12F).

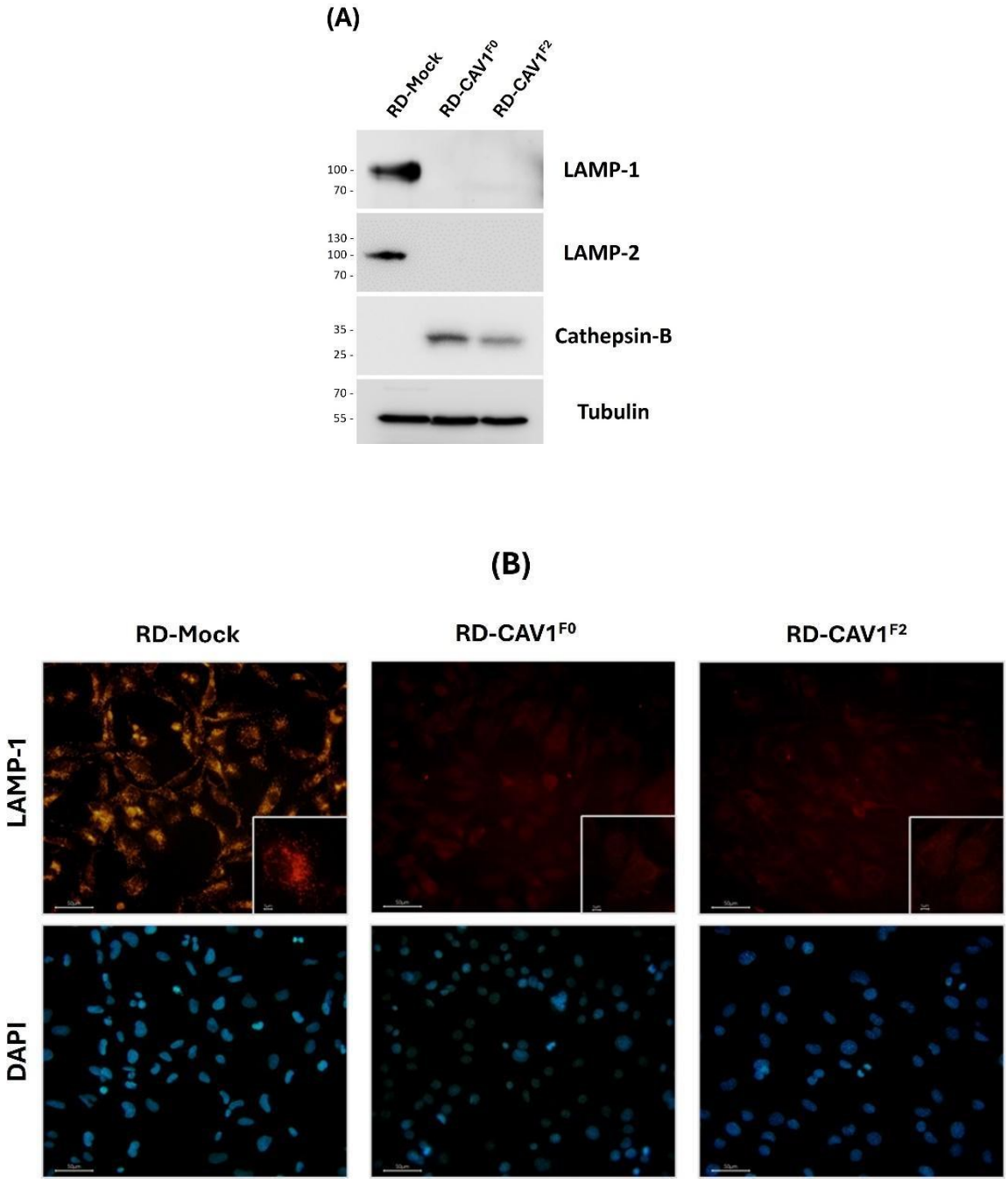
(A)
RD-Mock
RD-CAV1F0
RD-CAV1F2
100 -
70 -
LAMP-1
130 -
100 -
70 -
LAMP-2
35 -
25 -
Cathepsin-B
70 -
55 -
Tubulin
(B)
RD-Mock
RD-CAV1F0
RD-CAV1F2
LAMP-1
DAPI

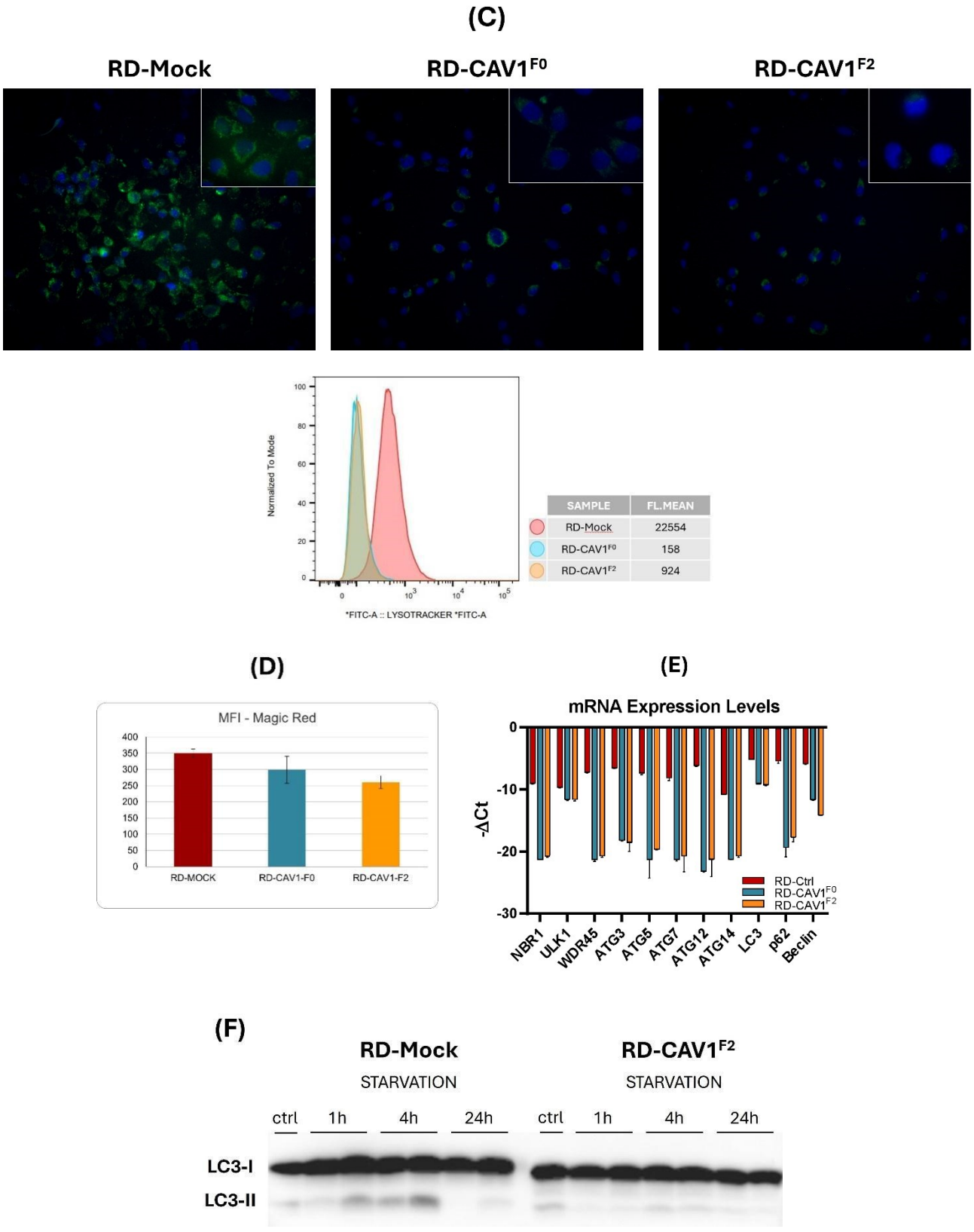

FIGURE 12. (A) Western blot analysis did not detect lysosomal associated protein LAMP-1 and LAMP-2 in RD-CAV1-cell bodies, which instead express cathepsin-B. (B) Immunostaining confirmed that LAMP-1 is less expressed in RD-CAV1^{F0} and RD-CAV1^{F2} cells compared to the

control. (C) Lysotracker staining showed less acidity in RD-CAV1 lysosomal compartments, suggesting less lysosomal activity, which has been confirmed by flow cytometry analysis. (D) Despite the detection of the protein by WB analysis, Magic Red assay demonstrated less cathepsin-B protease activity, corroborating with Lysotracker data. (E) *real-time* q-PCR showed less expression of ATG, LC3, NBR1, ULK1, WDR45, p62 and beclin mRNA expression levels and (F) starvation conditions demonstrated a decreased LC3-I / LC3-II conversion in RD-CAV1^{F2} cells compared to the RD-Mock. All these data suggest that Cav-1 overexpression affects lysosomal activity inducing autophagy impairment.

Taken together, these data demonstrate that Cav-1 overexpression causes an impairment in the lysosomal activity and at the same time increases the endosomal intracellular trafficking, promoting the MVB fusion with the plasma membrane rather than with lysosomes for the degradation, leading to a significantly higher *s*EV release in these cells.

4.6. RD cells overexpressing caveolin-1 release vesicles that modulate the tumour microenvironment

It is well known that EVs are involved in the process of tumour progression and since they are released by all cells for intercellular communication, it's easy to figure out that cancer-derived EVs can have an effect on the tumour microenvironment [168–170]. Many studies have demonstrated the ability of cancer-derived EVs to enhance the development of a metastatic tumour niche as well as the evasion of the immune system [171–173]. For this reason, and considering both the high metastatic potential of RD cells overexpressing Cav-1 and their altered vesicular secretome, we employed the RD-derived EVs for the treatment of HUVECs (human endothelial cell line) and THP-1 (human monocytic cell line).

4.6.1. RD-CAV1 *s*EVs induce migration and proliferation in HUVECs

It has already been demonstrated that Cav-1 overexpression in RD cells promotes the development of malignant features, including metastasis formation through Erk

pathway hyperactivation [72]. Given the deep alterations of the vesicular secretome in RD cells overexpressing Cav-1 we decided to investigate whether RD-EVs may be involved in the process of RD dissemination. The exo-free FBS conditioned media obtained from RD-Mock and RD-CAV1^{F2} cells were centrifuged as previously described to obtain *s*EV subpopulation; the derived supernatants were then concentrated with 10 kDa membrane to obtain concentrated total proteins. HUVECs were first treated in a transwell migration assay with three different concentrations of total proteins which demonstrated to be not cytotoxic (data not shown). After 24 h of co-incubation, RD-CAV1^{F2}-derived proteins have enhanced endothelial migration more than RD-Mock ones; in particular, the 100 ug/ml condition induced a significantly higher stimulation compared to the control (Fig. 13A).

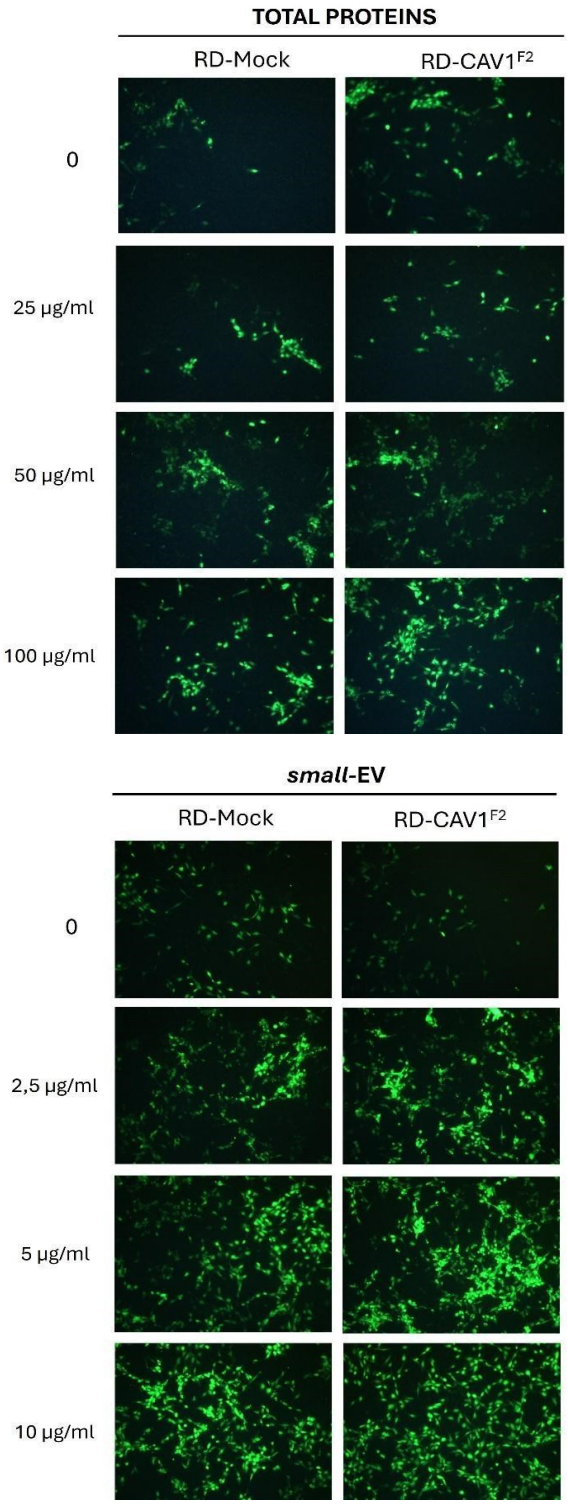
TOTAL PROTEINS
RD-Mock
RD-CAV1F2
0
25 µg/ml
50 µg/ml
100 µg/ml

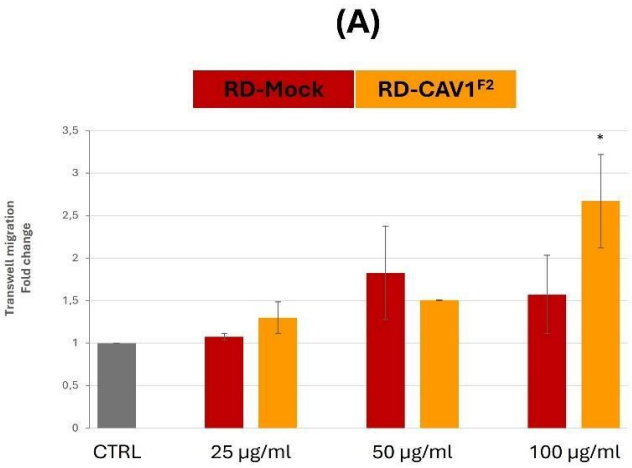
(A)
RD-Mock
RD-CAV1F2
Transwell migration
Fold change
3,5
3
2,5
2
1,5
1
0,5
0
*
CTRL
25 µg/ml
50 µg/ml
100 µg/ml

small-EV
RD-Mock
RD-CAV1F2
0
2,5 µg/ml
5 µg/ml
10 µg/ml

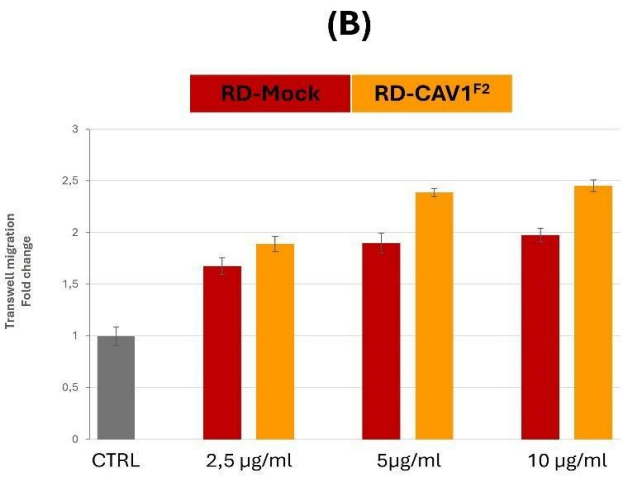
(B)
RD-Mock
RD-CAV1F2
Transwell migration
Fold change
3
2,5
2
1,5
1
0,5
0
CTRL
2,5 µg/ml
5µg/ml
10 µg/ml

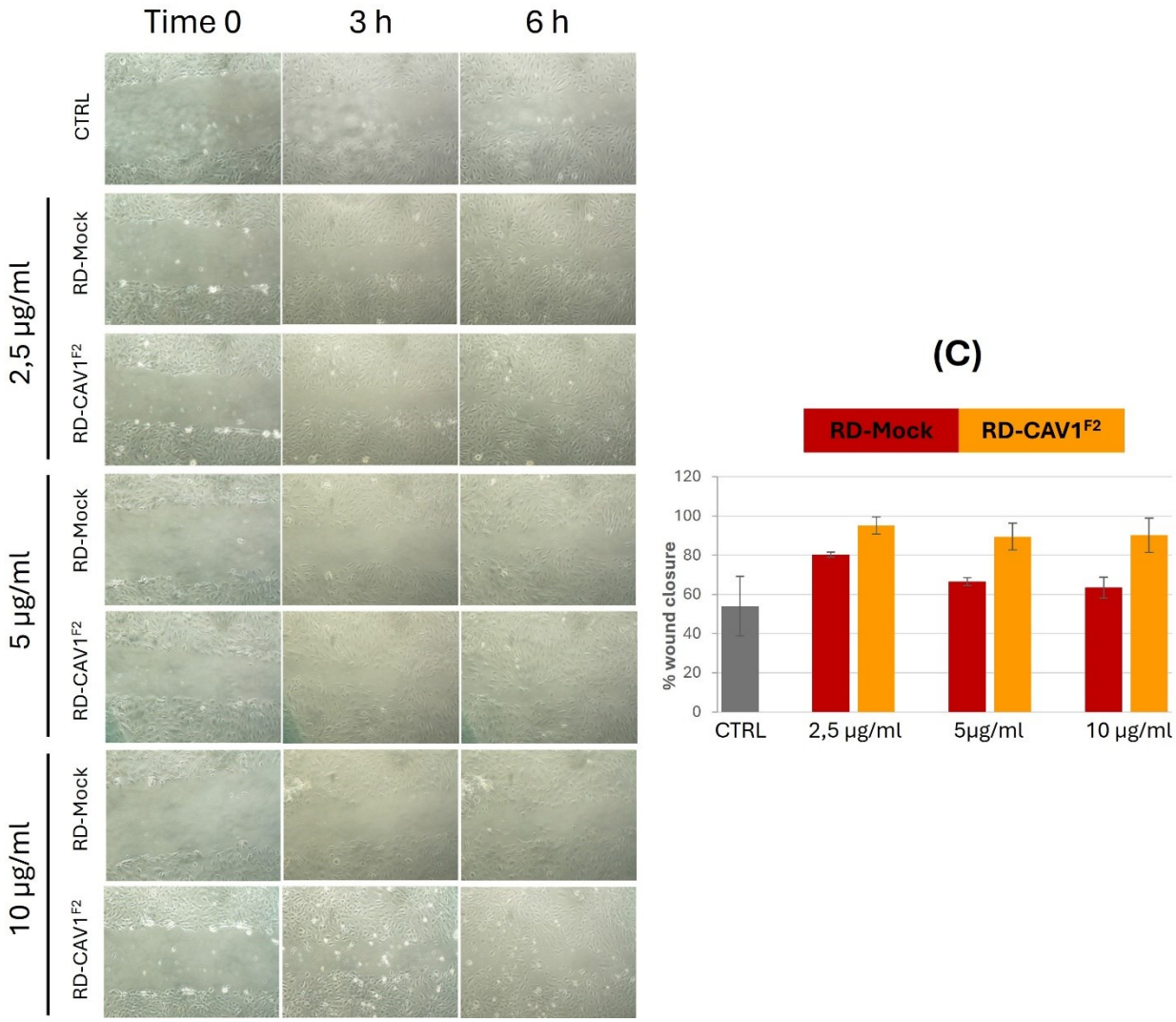

FIGURE 13. (A) Transwell migration assay showed that RD-CAV1^{F2}-derived total proteins increased HUVEC migration, particularly at 100 µg/ml. (B) Transwell migration assay performed with purified *s*EV subpopulation demonstrated that RD-CAV1^{F2}-derived *s*EVs increased HUVEC migration more than RD-Mock for all the tested concentrations. (C) RD-Mock and RD-CAV1^{F2}-derived *s*EVs were also employed in the wound healing assay showing that the percentage of wound closure is higher for HUVECs treated with RD-CAV1^{F2}-derived *s*EVs for all the tested concentrations.

The same treatment has been subsequently performed with the subpopulation of purified *s*EV: RD-CAV1^{F2} -derived *s*EV demonstrated to be more effective in stimulating HUVEC migration after 24 h of co-incubation in all the tested concentrations (Fig. 13B). RD-derived *s*EV have been also employed for the wound healing assay, in which the

percentage of wound closure is always higher in HUVECs treated with RD-CAV1^{F2} derived *s*EV compared to the control (Fig. 13C).

Taken together these data demonstrate that *s*EVs have a role in determining the metastatic behaviour of RD-cells overexpressing Cav-1, giving their contribution by increasing endothelial cell migration and proliferation.

4.6.2. RD-CAV1 *s*EVs alter cytokine expression in THP-1 cells

THP-1, a cellular model of human macrophage precursor monocytes, were plated in a 24-well plate (1x10^6 cells/ml) and treated with RD-Mock- and RD-CAV1^{F2}-derived *s*EVs. After 6 h and 24 h of co-incubation THP-1 treated cells were collected and subjected to RNA extraction and *real-time* q-PCR. In Fig. 14 we reported the THP-1 expression levels of the typical pro- and anti-inflammatory cytokines IL-1β, IL-6 and IL-10, respectively. We demonstrated that after 6 h treatment there are no relevant differences between RD-Mock and RD-CAV1^{F2} in the effects on the cytokine expression levels, whereas at 24 h RD-CAV1^{F2}-derived *s*EVs increase the expression of the pro-inflammatory cytokines IL-1β and IL-6 compared to the RD-Mock ones. But the most interesting result regards the IL-10 expression levels which increase more than twofold at 24 h with RD-CAV1^{F2}-derived *s*EVs. IL-10 is an anti-inflammatory cytokine whose levels are found to be high in macrophages with M2-phenotype known as TAMs (tumour-associated macrophages) [174].

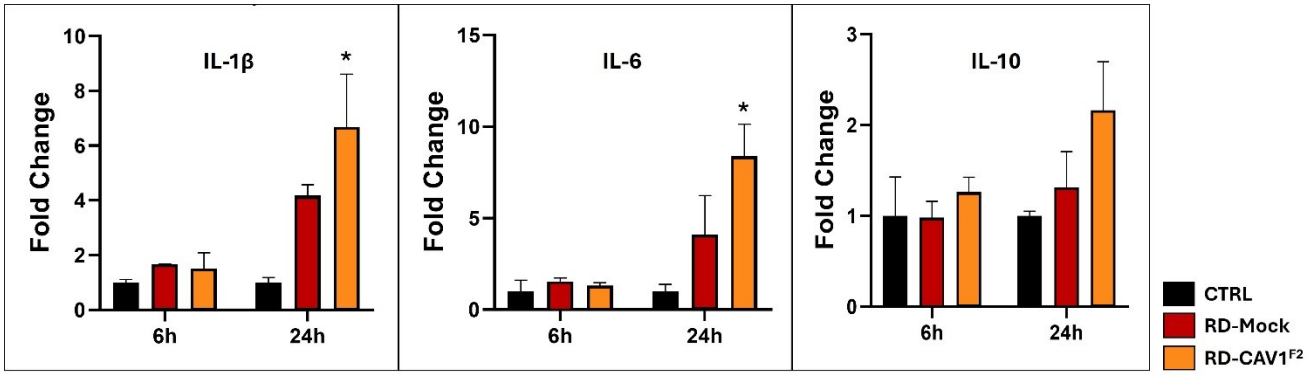

FIGURE 14. *real time* q-PCR demonstrated that treatment with RD-CAV1^{F2}-derived *s*EVs increased pro-inflammatory cytokine IL-1β and IL-6 expression in THP-1 at 6 h, and particularly at 24 h. Also anti-inflammatory cytokine IL-10 expression levels start to increase at 24 h with RD-CAV1^{F2}-derived *s*EVs, suggesting their potential ability to promote the development of a TAMs-like phenotype.

Physiologically, macrophages shift from a pro-inflammatory (M1) to an anti-inflammatory (M2) state to balance inflammation and regeneration. However, in the tumour niche there's a high M2/M1 ratio in TAMs, which avoids the recruitment of the other immune cells promoting a poor prognosis in most solid tumours [175]. We demonstrated that in our model, Cav-1 overexpression enhances the delivery of vesicles that after 24 h of treatment start to promote the expression of the anti-inflammatory cytokine IL-10 in THP-1 cells, paving the way for the possibility of considering these vesicles able to affect and elude the immune system.

5. DISCUSSION

The present study is built on the established role of Cav-1 overexpression as a tumour enhancer in the *in vitro* rhabdomyosarcoma model (RD), in which Codenotti et al demonstrated its contribution to tumour growth and metastatic potential [72]. Despite its controversial role in tumour progression [23], many studies showed that Cav-1 acts as an oncoprotein in a variety of cancers [39], including rhabdomyosarcoma in which Cav-1 is found to be a marker of poor differentiation [44]. Furthermore, Cav-1 is located in strategic areas of the phospholipid bilayer, such as caveolae and lipid rafts, which are involved in the intracellular and extracellular vesicular trafficking [17]. Extracellular vesicles (EV) are lipid-bound vesicles released by all types of cells for cell-to-cell communication [176]; cancer cells release EVs as a "tool" for spreading malignancy since their composition reflects the one of their cells of origin [177,178].

Since RD-cells overexpressing Cav-1 show typical malignant features such as chemoresistance [70], increased invasiveness [72] and radioresistance [74], and since Cav-1 was found to be directly involved in the regulation of EV biogenesis and cargo sorting [22], we aimed to assess if Cav-1 overexpression has an impact on the EV machinery in RD cell model. By SEM, TEM (Fig. 6) and NTA (Fig. 7A-B) analyses we demonstrated that Cav-1 overexpressing cells release a higher amount of small-EVs (*s*EV), with a completely different protein composition compared to the control (RD-Mock). The proteomic analysis found that Cav-1 induces an alteration in *s*EV protein cargo, leading to the release of more but emptier vesicles (Fig 10A-B). All the EV characterization methods employed in this study including western blot (Fig. 8A, 8C), flow cytometry (Fig. 9C) and proteomic analyses (Fig. 10C), showed that the RD-CAV1-derived *s*EVs are characterized by the downregulation of the typical *s*EV tetraspanin CD63, CD9 and CD81. Given the importance of these tetraspanins, in particular of CD63, in *s*EV biogenesis and cargo sorting [153] and given their low expression levels also in the RD cell bodies (Fig. 9A-B), we evaluated their mRNA levels, revealing no significative differences compared to the control (Fig.9D). These findings indicate that other factors, such as miRNA, might be involved in this mechanism instead of gene loss,

which are already planned to be further explored. It is important to emphasise that RD-CAV1-derived *s*EVs still express other *s*EV makers like ALIX and TSG-101 (Fig. 8A, 8C) that are well-known players in *s*EV biogenesis [179], which combined with the TEM analysis and ExoBrite staining, confirms their nature despite the CD-downregulation.

In order to better understand the increased release of such different vesicles from RD cells overexpressing CAV-1 we explored the intracellular vesicular trafficking from which *s*EVs directly originate. We first found that Rab proteins, which are well-established regulators of vesicle trafficking [180], are always more expressed in RD-CAV1 cells compared to the control (Fig. 11A), as well as LBPA (Fig. 11B higher panel) and Syntenin-1 (Fig. 11B lower panel). This data corroborates with the one obtained from the endosomal characterization, in which RD-CAV1-derived LEs exhibit higher levels of Rab7 and lower levels of CD63 and CD81, as expected (Fig. 11C). Moreover, live-cell imaging revealed that RD cells overexpressing Cav-1 internalize a higher amount of exogenous dextran in a shorter time through the endosomal pathway [161] compared to RD-Mock cells (Fig. 11D). Lastly, WB analysis performed on the endosomal fractions of the three cell lines also revealed that LAMP2A expression levels are progressively reduced from RD-Mock to RD-CAV1^{F2} samples (Fig. 11C). Since LAMP2A is demonstrated to be responsible for KFERQ-protein loading into ILVs [117], and since HIST-H3 (a nuclear protein containing KFERQ-motif) was less detected in the endosomal fraction of CAV1-overexpressing samples, LAMP2A decrease could be one of the mechanisms involved in the overall decreased protein cargo in this model. Taken together, all these data demonstrate that behind the increased *s*EV release in RD-cells overexpressing Cav-1 there is an increased intracellular vesicular trafficking and that the altered *s*EV protein composition reflects the deep alterations of both cellular and endosomal protein pattern, starting from the downregulation of some key protein sorting players like CD63 and LAMP2A [117,153].

Recent studies demonstrated that Cav-1 overexpression can inhibit autophagy [181] and that conversely this mechanism can be enhanced by Cav-1 knockdown [182]. In our RD model, we found that Cav-1 overexpression induces an impairment in lysosomal

functions. Both LAMP-1 and LAMP-2 proteins (Fig. 12A-B), as well as ATG gene expression levels (Fig. 12E), are found to be lower in RD-CAV1^{F0} and RD-CAV1^{F2} cells compared to the control. Cathepsin-D was detected by WB analysis (Fig. 12A) but Magic Red measured less protease activity in Cav-1 overexpressing cells (Fig. 12D). The same outcome has been obtained by Lysotracker staining, detecting low acidity degree in RD-CAV1^{F0} and RD-CAV1^{F2} cells compared to RD-Mock (Fig. 12C). Moreover, monitoring autophagy flux by inducing cell starvation up to 24 h, we found that LC3-I / LC3-II conversion is higher in RD-Mock at each time-point (Fig. 12F). Since LC3-II levels are directly correlated with the number of autophagosomes and autophagy-related structures [183], we can speculate that Cav-1 overexpression induces a decrease in degradation processes. Emerging evidence proposes that mature MVBs may not only fuse with the plasma membrane for the release or with lysosomes for degradation, but also with autophagosomes that can be released outwards as "amphiectosomes" [184]. In the RD-model we can exclude that this mechanism could be relevant in determining the increased EV release since Cav-1 overexpression critically affects the autophagy machinery.

Lastly, we demonstrated that the altered vesicular secretome contributes to promoting the aggressiveness of RD cells overexpressing Cav-1. RD-CAV1^{F2}-derived *s*EVs increase HUVEC proliferation and migration (Fig.13 A-C), suggesting their own metastatic potential. Moreover, they alter THP-1 cytokine expression by inducing an increase in pro-inflammatory IL-1β and IL-6 levels, but also an increase in anti-inflammatory IL-10 levels after 24 h of treatment (Fig. 14), suggesting that RD-CAV1^{F2}-derived *s*EVs might be able to induce phenotype transformation [175] thus favouring the immune system evasion.

6. CONCLUSIONS AND FUTURE PERSPECTIVES

To conclude, with the present work we demonstrated that Cav-1 overexpression critically modifies the EV machinery in the *in vitro* embryonal rhabdomyosarcoma model employed in this study, by promoting intracellular vesicular trafficking process, which added to the impairment in autophagic functions, led to an increased vesicle release. RD-CAV1-derived *s*EVs exhibit a completely different protein pattern and actively participate in modulating the tumour microenvironment, suggesting their contribution to RD-CAV1 cell aggressiveness.

Further studies will be conducted in order to complete RD-EV characterization such as lipid- and miRNA- profiling and to clarify the specific molecular mechanisms by which Cav-1 can introduce such deep alterations when overexpressed. First unpublished data obtained from lipidomic analysis (data not showed) highlight that RD-CAV1 cells and -*s*EVs exhibit a completely different lipidic profile compared to the RD-Mock ones, thus extending the ability of Cav-1 overexpression to induce deep alteration not only in the protein composition but also in the lipidic one. MiRNomic analysis will be useful in order to evaluate specific miRNA targeting CDs, which will might explain the different expression of these tetraspanins in RD-derived *s*EVs.

7. ACKNOWLEDGEMENTS

It’s a pleasure to thank first Prof. Michele Guescini for giving me the opportunity to start this path, and making me passionate about the world of research; he was determinant for my professional and personal education.

A special thanks also to Dr. Paola Ceccaroli and Dr. Emanuela Polidori who are part of the Guescini’s research group; thanks to their knowledge and expertise it was possible for me to do this work and grow professionally.

Special thanks also to Dr. Serena Maggio, the person who most of all passed on knowledge, love, and dedication for this job to me.

Finally, thanks to all the external collaborators from the University of Urbino, Ancona, Brescia, Perugia, and Bologna for their contribution to this research work.

8. REFERENCES

1. Williams, T.M.; Lisanti, M.P. The Caveolin Proteins. *Genome Biol* 2004, *5*, 214, doi:10.1186/gb-2004-5-3-214.

2. Simons, K.; Toomre, D. Lipid Rafts and Signal Transduction. *Nat Rev Mol Cell Biol* 2000, *1*, 31–39, doi:10.1038/35036052.

3. Brown, D.A.; London, E. Functions of lipid rafts in biological membranes. *Annu Rev Cell Dev Biol* 1998, *14*, 111–136, doi:10.1146/annurev.cellbio.14.1.111.

4. Galbiati, F.; Razani, B.; Lisanti, M.P. Emerging Themes in Lipid Rafts and Caveolae. *Cell* 2001, *106*, 403–411, doi:10.1016/S0092-8674(01)00472-X.

5. Liu, J.; Oh, P.; Horner, T.; Rogers, R.A.; Schnitzer, J.E. Organized Endothelial Cell Surface Signal Transduction in Caveolae Distinct from Glycosylphosphatidylinositol-Anchored Protein Microdomains. *Journal of Biological Chemistry* 1997, *272*, 7211–7222, doi:10.1074/jbc.272.11.7211.

6. Schlegel, A.; Arvan, P.; Lisanti, M.P. Caveolin-1 Binding to Endoplasmic Reticulum Membranes and Entry into the Regulated Secretory Pathway Are Regulated by Serine Phosphorylation. *Journal of Biological Chemistry* 2001, *276*, 4398–4408, doi:10.1074/jbc.M005448200.

7. Fielding, P.E.; Chau, P.; Liu, D.; Spencer, T.A.; Fielding, C.J. Mechanism of Platelet-Derived Growth Factor-Dependent Caveolin-1 Phosphorylation: Relationship to Sterol Binding and the Role of Serine-80. *Biochemistry* 2004, *43*, 2578–2586, doi:10.1021/bi035442c.

8. Kurzchalia, T. V; Dupree, P.; Parton, R.G.; Kellner, R.; Virta, H.; Lehnert, M.; Simons, K. VIP21, a 21-KD Membrane Protein Is an Integral Component of Trans-Golgi-Network-Derived Transport Vesicles. *J Cell Biol* 1992, *118*, 1003–1014, doi:10.1083/jcb.118.5.1003.

9. Liu, P.; Rudick, M.; Anderson, R.G.W. Multiple Functions of Caveolin-1. *Journal of Biological Chemistry* 2002, *277*, 41295–41298, doi:10.1074/jbc.R200020200.

10. Li, W.-P.; Liu, P.; Pilcher, B.K.; Anderson, R.G.W. Cell-Specific Targeting of Caveolin-1 to Caveolae, Secretory Vesicles, Cytoplasm or Mitochondria. *J Cell Sci* 2001, *114*, 1397–1408, doi:10.1242/jcs.114.7.1397.

11. Song, K.S.; Scherer, P.E.; Tang, Z.; Okamoto, T.; Li, S.; Chafel, M.; Chu, C.; Kohtz, D.S.; Lisanti, M.P. Expression of Caveolin-3 in Skeletal, Cardiac, and Smooth Muscle Cells.

Journal of Biological Chemistry 1996, *271*, 15160–15165, doi:10.1074/jbc.271.25.15160.

12. Pelkmans, L.; Helenius, A. Endocytosis Via Caveolae. *Traffic* 2002, *3*, 311–320, doi:10.1034/j.1600-0854.2002.30501.x.

13. Ariotti, N.; Rae, J.; Leneva, N.; Ferguson, C.; Loo, D.; Okano, S.; Hill, M.M.; Walser, P.; Collins, B.M.; Parton, R.G. Molecular Characterization of Caveolin-Induced Membrane Curvature. *Journal of Biological Chemistry* 2015, *290*, 24875–24890, doi:10.1074/jbc.M115.644336.

14. Krishna, A.; Prakash, S.; Sengupta, D. Sphingomyelin Effects in Caveolin-1 Mediated Membrane Curvature. *J Phys Chem B* 2020, *124*, 5177–5185, doi:10.1021/acs.jpcb.0c02962.

15. Yang, G.; Xu, H.; Li, Z.; Li, F. Interactions of Caveolin-1 Scaffolding and Intramembrane Regions Containing a CRAC Motif with Cholesterol in Lipid Bilayers. *Biochimica et Biophysica Acta (BBA) - Biomembranes* 2014, *1838*, 2588–2599, doi:10.1016/j.bbamem.2014.06.018.

16. Prakash, S.; Malshikare, H.; Sengupta, D. Molecular Mechanisms Underlying Caveolin-1 Mediated Membrane Curvature. *J Membr Biol* 2022, *255*, 225–236, doi:10.1007/s00232-022-00236-y.

17. Ouweneel, A.B.; Thomas, M.J.; Sorci-Thomas, M.G. The Ins and Outs of Lipid Rafts: Functions in Intracellular Cholesterol Homeostasis, Microparticles, and Cell Membranes. *J Lipid Res* 2020, *61*, 676–686, doi:10.1194/jlr.TR119000383.

18. Liu, P.; Li, W.-P.; Machleidt, T.; Anderson, R.G.W. Identification of Caveolin-1 in Lipoprotein Particles Secreted by Exocrine Cells. *Nat Cell Biol* 1999, *1*, 369–375, doi:10.1038/14067.

19. Logozzi, M.; De Milito, A.; Lugini, L.; Borghi, M.; Calabrò, L.; Spada, M.; Perdicchio, M.; Marino, M.L.; Federici, C.; Iessi, E.; et al. High Levels of Exosomes Expressing CD63 and Caveolin-1 in Plasma of Melanoma Patients. *PLoS One* 2009, *4*, e5219, doi:10.1371/journal.pone.0005219.

20. Lee, H.; Li, C.; Zhang, Y.; Zhang, D.; Otterbein, L.E.; Jin, Y. Caveolin-1 Selectively Regulates MicroRNA Sorting into Microvesicles after Noxious Stimuli. *Journal of Experimental Medicine* 2019, *216*, 2202–2220, doi:10.1084/jem.20182313.

21. Sawada, N.; Taketani, Y.; Amizuka, N.; Ichikawa, M.; Ogawa, C.; Nomoto, K.; Nashiki, K.; Sato, T.; Arai, H.; Isshiki, M.; et al. Caveolin-1 in Extracellular Matrix Vesicles Secreted from Osteoblasts. *Bone* 2007, *41*, 52–58, doi:10.1016/j.bone.2007.02.030.

22. Albacete-Albacete, L.; Navarro-Lérida, I.; López, J.A.; Martín-Padura, I.; Astudillo, A.M.; Ferrarini, A.; Van-Der-Heyden, M.; Balsinde, J.; Orend, G.; Vázquez, J.; et al. ECM Deposition Is Driven by Caveolin-1-Dependent Regulation of Exosomal Biogenesis and Cargo Sorting. *J Cell Biol* 2020, *219*, doi:10.1083/jcb.202006178.

23. Campos, A.; Burgos-Ravanal, R.; González, M.F.; Huilcaman, R.; Lobos González, L.; Quest, A.F.G. Cell Intrinsic and Extrinsic Mechanisms of Caveolin-1-Enhanced Metastasis. *Biomolecules* 2019, *9*, doi:10.3390/biom9080314.

24. Ni, K.; Wang, C.; Carnino, J.M.; Jin, Y. The Evolving Role of Caveolin-1: A Critical Regulator of Extracellular Vesicles. *Medical Sciences* 2020, *8*, 46, doi:10.3390/medsci8040046.

25. Zundel, W.; Giaccia, A. Inhibition of the Anti-Apoptotic PI(3)K/Akt/Bad Pathway by Stress. *Genes Dev* 1998, *12*, 1941–1946, doi:10.1101/gad.12.13.1941.

26. Zundel, W.; Swiersz, L.M.; Giaccia, A. Caveolin 1-Mediated Regulation of Receptor Tyrosine Kinase-Associated Phosphatidylinositol 3-Kinase Activity by Ceramide. *Mol Cell Biol* 2000, *20*, 1507–1514, doi:10.1128/MCB.20.5.1507-1514.2000.

27. Liu, J.; Lee, P.; Galbiati, F.; Kitsis, R.N.; Lisanti, M.P. Caveolin-1 Expression Sensitizes Fibroblastic and Epithelial Cells to Apoptotic Stimulation. *American Journal of Physiology-Cell Physiology* 2001, *280*, C823–C835, doi:10.1152/ajpcell.2001.280.4.C823.

28. Podar, K.; Tai, Y.-T.; Cole, C.E.; Hideshima, T.; Sattler, M.; Hamblin, A.; Mitsiades, N.; Schlossman, R.L.; Davies, F.E.; Morgan, G.J.; et al. Essential Role of Caveolae in Interleukin-6- and Insulin-like Growth Factor I-Triggered Akt-1-Mediated Survival of Multiple Myeloma Cells. *Journal of Biological Chemistry* 2003, *278*, 5794–5801, doi:10.1074/jbc.M208636200.

29. Li, L.; Ren, C.H.; Tahir, S.A.; Ren, C.; Thompson, T.C. Caveolin-1 Maintains Activated Akt in Prostate Cancer Cells through Scaffolding Domain Binding Site Interactions with and Inhibition of Serine/Threonine Protein Phosphatases PP1 and PP2A. *Mol Cell Biol* 2003, *23*, 9389–9404, doi:10.1128/MCB.23.24.9389-9404.2003.

30. Williams, T.M.; Lisanti, M.P. Caveolin-1 in Oncogenic Transformation, Cancer, and Metastasis. *American Journal of Physiology-Cell Physiology* 2005, *288*, C494–C506, doi:10.1152/ajpcell.00458.2004.

31. Racine, C.; Bélanger, M.; Hirabayashi, H.; Boucher, M.; Chakir, J.; Couet, J. Reduction of Caveolin 1 Gene Expression in Lung Carcinoma Cell Lines. *Biochem Biophys Res Commun* 1999, *255*, 580–586, doi:10.1006/bbrc.1999.0236.

32. Lee, S.W.; Reimer, C.L.; Oh, P.; Campbell, D.B.; Schnitzer, J.E. Tumor Cell Growth Inhibition by Caveolin Re-Expression in Human Breast Cancer Cells. *Oncogene* 1998, *16*, 1391–1397, doi:10.1038/sj.onc.1201661.

33. Torrejón, B.; Cristóbal, I.; Rojo, F.; García-Foncillas, J. Caveolin-1 Is Markedly Downregulated in Patients with Early-Stage Colorectal Cancer. *World J Surg* 2017, *41*, 2625–2630, doi:10.1007/s00268-017-4065-9.

34. Wiechen, K.; Diatchenko, L.; Agoulnik, A.; Scharff, K.M.; Schober, H.; Arlt, K.; Zhumabayeva, B.; Siebert, P.D.; Dietel, M.; Schäfer, R.; et al. Caveolin-1 Is Down-Regulated in Human Ovarian Carcinoma and Acts as a Candidate Tumor Suppressor Gene. *Am J Pathol* 2001, *159*, 1635–1643, doi:10.1016/S0002-9440(10)63010-6.

35. Wiechen, K.; Sers, C.; Agoulnik, A.; Arlt, K.; Dietel, M.; Schlag, P.M.; Schneider, U. Down-Regulation of Caveolin-1, a Candidate Tumor Suppressor Gene, in Sarcomas. *Am J Pathol* 2001, *158*, 833–839, doi:10.1016/S0002-9440(10)64031-X.

36. Manara, M.C.; Bernard, G.; Lollini, P.-L.; Nanni, P.; Zuntini, M.; Landuzzi, L.; Benini, S.; Lattanzi, G.; Sciandra, M.; Serra, M.; et al. CD99 Acts as an Oncosuppressor in Osteosarcoma. *Mol Biol Cell* 2006, *17*, 1910–1921, doi:10.1091/mbc.e05-10-0971.

37. Quann, K.; Gonzales, D.M.; Mercier, I.; Wang, C.; Sotgia, F.; Pestell, R.G.; Lisanti, M.P.; Jasmin, J.-F. Caveolin-1 Is a Negative Regulator of Tumor Growth in Glioblastoma and Modulates Chemosensitivity to Temozolomide. *Cell Cycle* 2013, *12*, 1510–1520, doi:10.4161/cc.24497.

38. Koleske, A.J.; Baltimore, D.; Lisanti, M.P. Reduction of Caveolin and Caveolae in Oncogenically Transformed Cells. *Proceedings of the National Academy of Sciences* 1995, *92*, 1381–1385, doi:10.1073/pnas.92.5.1381.

39. Wong, T.H.; Dickson, F.H.; Timmins, L.R.; Nabi, I.R. Tyrosine Phosphorylation of Tumor Cell Caveolin-1: Impact on Cancer Progression. *Cancer and Metastasis Reviews* 2020, *39*, 455–469, doi:10.1007/s10555-020-09892-9.

40. Han, Q.; Qiu, S.; Hu, H.; Li, W.; Li, X. Role of Caveolae Family-Related Proteins in the Development of Breast Cancer. *Front Mol Biosci* 2023, *10*, doi:10.3389/fmolb.2023.1242426.

41. Zhang, W.; Razani, B.; Altschuler, Y.; Bouzahzah, B.; Mostov, K.E.; Pestell, R.G.; Lisanti, M.P. Caveolin-1 Inhibits Epidermal Growth Factor-Stimulated Lamellipod Extension and Cell Migration in Metastatic Mammary Adenocarcinoma Cells (MTLn3). *Journal of Biological Chemistry* 2000, *275*, 20717–20725, doi:10.1074/jbc.M909895199.

42. Fiucci, G.; Ravid, D.; Reich, R.; Liscovitch, M. Caveolin-1 Inhibits Anchorage-Independent Growth, Anoikis and Invasiveness in MCF-7 Human Breast Cancer Cells. *Oncogene* 2002, *21*, 2365–2375, doi:10.1038/sj.onc.1205300.

43. Alevizos, L.; Kataki, A.; Derventzi, A.; Gomatos, I.; Loutraris, C.; Gloustianou, G.; Manouras, A.; Konstadoulakis, M.M.; Zografos, G. Breast Cancer Nodal Metastasis Correlates with Tumour and Lymph Node Methylation Profiles of Caveolin-1 and CXCR4. *Clin Exp Metastasis* 2014, *31*, 511–520, doi:10.1007/s10585-014-9645-6.

44. Rossi, S.; Poliani, P.L.; Cominelli, M.; Bozzato, A.; Vescovi, R.; Monti, E.; Fanzani, A. Caveolin 1 Is a Marker of Poor Differentiation in Rhabdomyosarcoma. *Eur J Cancer* 2011, *47*, 761–772, doi:10.1016/j.ejca.2010.10.018.

45. Li, L.; Zhang, K.; Lu, C.; Sun, Q.; Zhao, S.; Jiao, L.; Han, R.; Lin, C.; Jiang, J.; Zhao, M.; et al. Caveolin-1-Mediated STAT3 Activation Determines Electrotaxis of Human Lung Cancer Cells. *Oncotarget* 2017, *8*, 95741–95754, doi:10.18632/oncotarget.21306.

46. Ruan, H.; Li, X.; Yang, H.; Song, Z.; Tong, J.; Cao, Q.; Wang, K.; Xiao, W.; Xiao, H.; Chen, X.; et al. Enhanced Expression of Caveolin-1 Possesses Diagnostic and Prognostic Value and Promotes Cell Migration, Invasion and Sunitinib Resistance in the Clear Cell Renal Cell Carcinoma. *Exp Cell Res* 2017, *358*, 269–278, doi:10.1016/j.yexcr.2017.07.004.

47. Mao, X.; Wong, S.Y.S.; Tse, E.Y.T.; Ko, F.C.F.; Tey, S.K.; Yeung, Y.S.; Man, K.; Lo, R.C.-L.; Ng, I.O.-L.; Yam, J.W.P. Mechanisms through Which Hypoxia-Induced Caveolin-1 Drives Tumorigenesis and Metastasis in Hepatocellular Carcinoma. *Cancer Res* 2016, *76*, 7242–7253, doi:10.1158/0008-5472.CAN-16-1031.

48. Ortiz, R.; Díaz, J.; Díaz, N.; Lobos-Gonzalez, L.; Cárdenas, A.; Contreras, P.; Díaz, M.I.; Otte, E.; Cooper-White, J.; Torres, V.; et al. Extracellular Matrix-Specific Caveolin-1 Phosphorylation on Tyrosine 14 Is Linked to Augmented Melanoma Metastasis but Not Tumorigenesis. *Oncotarget* 2016, *7*, 40571–40593, doi:10.18632/oncotarget.9738.

49. Lagares-Tena, L.; García-Monclús, S.; López-Alemany, R.; Almacellas-Rabaiget, O.; Huertas-Martínez, J.; Sáinz-Jaspeado, M.; Mateo-Lozano, S.; Rodríguez-Galindo, C.; Rello-Varona, S.; Herrero-Martín, D.; et al. Caveolin-1 Promotes Ewing Sarcoma Metastasis Regulating MMP-9 Expression through MAPK/ERK Pathway. *Oncotarget* 2016, *7*, 56889–56903, doi:10.18632/oncotarget.10872.

50. PDQ Pediatric Treatment Editorial Board *Childhood Rhabdomyosarcoma Treatment (PDQ®): Health Professional Version*; 2002.

51. Anderson, J.; Gordon, A.; McManus, A.; Shipley, J.; Pritchard-Jones, K. Disruption of Imprinted Genes at Chromosome Region 11p15.5 in Paediatric Rhabdomyosarcoma. *Neoplasia* 1999, *1*, 340–348, doi:10.1038/sj.neo.7900052.

52. Shern, J.F.; Chen, L.; Chmielecki, J.; Wei, J.S.; Patidar, R.; Rosenberg, M.; Ambrogio, L.; Auclair, D.; Wang, J.; Song, Y.K.; et al. Comprehensive Genomic Analysis of Rhabdomyosarcoma Reveals a Landscape of Alterations Affecting a Common Genetic

Axis in Fusion-Positive and Fusion-Negative Tumors. *Cancer Discov* 2014, *4*, 216–231, doi:10.1158/2159-8290.CD-13-0639.

53. Marampon, F.; Ciccarelli, C.; Zani, B.M. Down-Regulation of c-Myc Following MEK/ERK Inhibition Halts the Expression of Malignant Phenotype in Rhabdomyosarcoma and in Non Muscle-Derived Human Tumors. *Mol Cancer* 2006, *5*, 31, doi:10.1186/1476-4598-5-31.

54. Marampon, F.; Bossi, G.; Ciccarelli, C.; Di Rocco, A.; Sacchi, A.; Pestell, R.G.; Zani, B.M. MEK/ERK Inhibitor U0126 Affects *in Vitro* and *in Vivo* Growth of Embryonal Rhabdomyosarcoma. *Mol Cancer Ther* 2009, *8*, 543–551, doi:10.1158/1535-7163.MCT-08-0570.

55. Marampon, F.; Gravina, G.L.; Di Rocco, A.; Bonfili, P.; Di Staso, M.; Fardella, C.; Polidoro, L.; Ciccarelli, C.; Festuccia, C.; Popov, V.M.; et al. MEK/ERK Inhibitor U0126 Increases the Radiosensitivity of Rhabdomyosarcoma Cells *In Vitro* and *In Vivo* by Downregulating Growth and DNA Repair Signals. *Mol Cancer Ther* 2011, *10*, 159–168, doi:10.1158/1535-7163.MCT-10-0631.

56. Gravina, G.L.; Festuccia, C.; Popov, V.M.; Di Rocco, A.; Colapietro, A.; Sanità, P.; Monache, S.D.; Musio, D.; De Felice, F.; Di Cesare, E.; et al. C-Myc Sustains Transformed Phenotype and Promotes Radioresistance of Embryonal Rhabdomyosarcoma Cell Lines. *Radiat Res* 2016, *185*, 411–422, doi:10.1667/RR14237.1.

57. Ciccarelli, C.; Vulcano, F.; Milazzo, L.; Gravina, G.L.; Marampon, F.; Macioce, G.; Giampaolo, A.; Tombolini, V.; Di Paolo, V.; Hassan, H.J.; et al. Key Role of MEK/ERK Pathway in Sustaining Tumorigenicity and in Vitro Radioresistance of Embryonal Rhabdomyosarcoma Stem-like Cell Population. *Mol Cancer* 2016, *15*, 16, doi:10.1186/s12943-016-0501-y.

58. Saini, M.; Verma, A.; Mathew, S.J. SPRY2 Is a Novel MET Interactor That Regulates Metastatic Potential and Differentiation in Rhabdomyosarcoma. *Cell Death Dis* 2018, *9*, 237, doi:10.1038/s41419-018-0261-2.

59. Barr, F.G.; Galili, N.; Holick, J.; Biegel, J.A.; Rovera, G.; Emanuel, B.S. Rearrangement of the PAX3 Paired Box Gene in the Paediatric Solid Tumour Alveolar Rhabdomyosarcoma. *Nat Genet* 1993, *3*, 113–117, doi:10.1038/ng0293-113.

60. Ognjanovic, S.; Linabery, A.M.; Charbonneau, B.; Ross, J.A. Trends in Childhood Rhabdomyosarcoma Incidence and Survival in the United States, 1975-2005. *Cancer* 2009, *115*, 4218–4226, doi:10.1002/cncr.24465.

61. Crist, W.; Gehan, E.A.; Ragab, A.H.; Dickman, P.S.; Donaldson, S.S.; Fryer, C.; Hammond, D.; Hays, D.M.; Herrmann, J.; Heyn, R. The Third Intergroup

Rhabdomyosarcoma Study. *Journal of Clinical Oncology* 1995, *13*, 610–630, doi:10.1200/JCO.1995.13.3.610.

62. Casanova, M.; Meazza, C.; Favini, F.; Fiore, M.; Morosi, C.; Ferrari, A. RHABDOMYOSARCOMA OF THE EXTREMITIES: A Focus on Tumors Arising in the Hand and Foot. *Pediatr Hematol Oncol* 2009, *26*, 321–331, doi:10.1080/08880010902964367.

63. Maurer, H.M.; Gehan, E.A.; Beltangady, M.; Crist, W.; Dickman, P.S.; Donaldson, S.S.; Fryer, C.; Hammond, D.; Hays, D.M.; Herrmann, J.; et al. The Intergroup Rhabdomyosarcoma Study-II. *Cancer* 1993, *71*, 1904–1922, doi:10.1002/1097-0142(19930301)71:5<1904::AID-CNCR2820710530>3.0.CO;2-X.

64. Trahair, T.; Andrews, L.; Cohn, R.J. Recognition of Li Fraumeni Syndrome at Diagnosis of a Locally Advanced Extremity Rhabdomyosarcoma. *Pediatr Blood Cancer* 2007, *48*, 345–348, doi:10.1002/pbc.20795.

65. Doros, L.; Yang, J.; Dehner, L.; Rossi, C.T.; Skiver, K.; Jarzembowski, J.A.; Messinger, Y.; Schultz, K.A.; Williams, G.; André, N.; et al. DICER1 Mutations in Embryonal Rhabdomyosarcomas from Children with and without Familial PPB-tumor Predisposition Syndrome. *Pediatr Blood Cancer* 2012, *59*, 558–560, doi:10.1002/pbc.24020.

66. Crucis, A.; Richer, W.; Brugières, L.; Bergeron, C.; Marie-Cardine, A.; Stephan, J.-L.; Girard, P.; Corradini, N.; Munzer, M.; Lacour, B.; et al. Rhabdomyosarcomas in Children with Neurofibromatosis Type I: A National Historical Cohort. *Pediatr Blood Cancer* 2015, *62*, 1733–1738, doi:10.1002/pbc.25556.

67. Ognjanovic, S.; Carozza, S.E.; Chow, E.J.; Fox, E.E.; Horel, S.; McLaughlin, C.C.; Mueller, B.A.; Puumala, S.; Reynolds, P.; Von Behren, J.; et al. Birth Characteristics and the Risk of Childhood Rhabdomyosarcoma Based on Histological Subtype. *Br J Cancer* 2010, *102*, 227–231, doi:10.1038/sj.bjc.6605484.

68. Chen, X.; Stewart, E.; Shelat, A.A.; Qu, C.; Bahrami, A.; Hatley, M.; Wu, G.; Bradley, C.; McEvoy, J.; Pappo, A.; et al. Targeting Oxidative Stress in Embryonal Rhabdomyosarcoma. *Cancer Cell* 2013, *24*, 710–724, doi:10.1016/j.ccr.2013.11.002.

69. Rossi, S.; Poliani, P.L.; Missale, C.; Monti, E.; Fanzani, A. Caveolins in Rhabdomyosarcoma. *J Cell Mol Med* 2011, *15*, 2553–2568, doi:10.1111/j.1582-4934.2011.01364.x.

70. Faggi, F.; Mitola, S.; Sorci, G.; Riuzzi, F.; Donato, R.; Codenotti, S.; Poliani, P.L.; Cominelli, M.; Vescovi, R.; Rossi, S.; et al. Phosphocaveolin-1 Enforces Tumor Growth and Chemoresistance in Rhabdomyosarcoma. *PLoS One* 2014, *9*, e84618, doi:10.1371/journal.pone.0084618.

71. Faggi, F.; Chiarelli, N.; Colombi, M.; Mitola, S.; Ronca, R.; Madaro, L.; Bouche, M.; Poliani, P.L.; Vezzoli, M.; Longhena, F.; et al. Cavin-1 and Caveolin-1 Are Both Required to Support Cell Proliferation, Migration and Anchorage-Independent Cell Growth in Rhabdomyosarcoma. *Laboratory Investigation* 2015, *95*, 585–602, doi:10.1038/labinvest.2015.45.

72. Codenotti, S.; Faggi, F.; Ronca, R.; Chiodelli, P.; Grillo, E.; Guescini, M.; Megiorni, F.; Marampon, F.; Fanzani, A. Caveolin-1 Enhances Metastasis Formation in a Human Model of Embryonal Rhabdomyosarcoma through Erk Signaling Cooperation. *Cancer Lett* 2019, *449*, 135–144, doi:10.1016/j.canlet.2019.02.013.

73. Park, J.-I. MAPK-ERK Pathway. *Int J Mol Sci* 2023, *24*, 9666, doi:10.3390/ijms24119666.

74. Codenotti, S.; Marampon, F.; Triggiani, L.; Bonù, M.L.; Magrini, S.M.; Ceccaroli, P.; Guescini, M.; Gastaldello, S.; Tombolini, V.; Poliani, P.L.; et al. Caveolin-1 Promotes Radioresistance in Rhabdomyosarcoma through Increased Oxidative Stress Protection and DNA Repair. *Cancer Lett* 2021, *505*, 1–12, doi:10.1016/j.canlet.2021.02.005.

75. Couch, Y.; Buzàs, E.I.; Di Vizio, D.; Gho, Y.S.; Harrison, P.; Hill, A.F.; Lötvall, J.; Raposo, G.; Stahl, P.D.; Théry, C.; et al. A Brief History of Nearly EV-erything – The Rise and Rise of Extracellular Vesicles. *J Extracell Vesicles* 2021, *10*, doi:10.1002/jev2.12144.

76. CHARGAFF, E.; WEST, R. The Biological Significance of the Thromboplastic Protein of Blood. *J Biol Chem* 1946, *166*, 189–197.

77. Wolf, P. The Nature and Significance of Platelet Products in Human Plasma. *Br J Haematol* 1967, *13*, 269–288, doi:10.1111/j.1365-2141.1967.tb08741.x.

78. Frühbeis, C.; Fröhlich, D.; Krämer-Albers, E.-M. Emerging Roles of Exosomes in Neuron–Glia Communication. *Front Physiol* 2012, *3*, doi:10.3389/fphys.2012.00119.

79. Marcilla, A.; Trelis, M.; Cortés, A.; Sotillo, J.; Cantalapiedra, F.; Minguez, M.T.; Valero, M.L.; Sánchez del Pino, M.M.; Muñoz-Antoli, C.; Toledo, R.; et al. Extracellular Vesicles from Parasitic Helminths Contain Specific Excretory/Secretory Proteins and Are Internalized in Intestinal Host Cells. *PLoS One* 2012, *7*, e45974, doi:10.1371/journal.pone.0045974.

80. Luga, V.; Zhang, L.; Viloria-Petit, A.M.; Ogunjimi, A.A.; Inanlou, M.R.; Chiu, E.; Buchanan, M.; Hosein, A.N.; Basik, M.; Wrana, J.L. Exosomes Mediate Stromal Mobilization of Autocrine Wnt-PCP Signaling in Breast Cancer Cell Migration. *Cell* 2012, *151*, 1542–1556, doi:10.1016/j.cell.2012.11.024.

81. Regev-Rudzki, N.; Wilson, D.W.; Carvalho, T.G.; Sisquella, X.; Coleman, B.M.; Rug, M.; Bursac, D.; Angrisano, F.; Gee, M.; Hill, A.F.; et al. Cell-Cell Communication between Malaria-Infected Red Blood Cells via Exosome-like Vesicles. *Cell* 2013, *153*, 1120–1133, doi:10.1016/j.cell.2013.04.029.

82. Barteneva, N.S.; Maltsev, N.; Vorobjev, I.A. Microvesicles and Intercellular Communication in the Context of Parasitism. *Front Cell Infect Microbiol* 2013, *3*, doi:10.3389/fcimb.2013.00049.

83. Mulcahy, L.A.; Pink, R.C.; Carter, D.R.F. Routes and Mechanisms of Extracellular Vesicle Uptake. *J Extracell Vesicles* 2014, *3*, doi:10.3402/jev.v3.24641.

84. Henderson, M.C.; Azorsa, D.O. The Genomic and Proteomic Content of Cancer Cell-Derived Exosomes. *Front Oncol* 2012, *2*, doi:10.3389/fonc.2012.00038.

85. Théry, C.; Zitvogel, L.; Amigorena, S. Exosomes: Composition, Biogenesis and Function. *Nat Rev Immunol* 2002, *2*, 569–579, doi:10.1038/nri855.

86. Baj-Krzyworzeka, M.; Szatanek, R.; Węglarczyk, K.; Baran, J.; Urbanowicz, B.; Brański, P.; Ratajczak, M.Z.; Zembala, M. Tumour-Derived Microvesicles Carry Several Surface Determinants and MRNA of Tumour Cells and Transfer Some of These Determinants to Monocytes. *Cancer Immunology, Immunotherapy* 2006, *55*, 808–818, doi:10.1007/s00262-005-0075-9.

87. Ratajczak, J.; Miekus, K.; Kucia, M.; Zhang, J.; Reca, R.; Dvorak, P.; Ratajczak, M.Z. Embryonic Stem Cell-Derived Microvesicles Reprogram Hematopoietic Progenitors: Evidence for Horizontal Transfer of MRNA and Protein Delivery. *Leukemia* 2006, *20*, 847–856, doi:10.1038/sj.leu.2404132.

88. Skog, J.; Würdinger, T.; van Rijn, S.; Meijer, D.H.; Gainche, L.; Curry, W.T.; Carter, B.S.; Krichevsky, A.M.; Breakefield, X.O. Glioblastoma Microvesicles Transport RNA and Proteins That Promote Tumour Growth and Provide Diagnostic Biomarkers. *Nat Cell Biol* 2008, *10*, 1470–1476, doi:10.1038/ncb1800.

89. Akers, J.C.; Gonda, D.; Kim, R.; Carter, B.S.; Chen, C.C. Biogenesis of Extracellular Vesicles (EV): Exosomes, Microvesicles, Retrovirus-like Vesicles, and Apoptotic Bodies. *J Neurooncol* 2013, *113*, 1–11, doi:10.1007/s11060-013-1084-8.

90. Abels, E.R.; Breakefield, X.O. Introduction to Extracellular Vesicles: Biogenesis, RNA Cargo Selection, Content, Release, and Uptake. *Cell Mol Neurobiol* 2016, *36*, 301–312, doi:10.1007/s10571-016-0366-z.

91. Bebelman, M.P.; Smit, M.J.; Pegtel, D.M.; Baglio, S.R. Biogenesis and Function of Extracellular Vesicles in Cancer. *Pharmacol Ther* 2018, *188*, 1–11, doi:10.1016/j.pharmthera.2018.02.013.

92. Théry, C.; Witwer, K.W.; Aikawa, E.; Alcaraz, M.J.; Anderson, J.D.; Andriantsitohaina, R.; Antoniou, A.; Arab, T.; Archer, F.; Atkin-Smith, G.K.; et al. Minimal Information for Studies of Extracellular Vesicles 2018 (MISEV2018): A Position Statement of the International Society for Extracellular Vesicles and Update of the MISEV2014 Guidelines. *J Extracell Vesicles* 2018, *7*, doi:10.1080/20013078.2018.1535750.

93. Hugel, B.; Martínez, M.C.; Kunzelmann, C.; Freyssinet, J.-M. Membrane Microparticles: Two Sides of the Coin. *Physiology (Bethesda)* 2005, *20*, 22–27, doi:10.1152/physiol.00029.2004.

94. Muralidharan-Chari, V.; Clancy, J.; Plou, C.; Romao, M.; Chavrier, P.; Raposo, G.; D'Souza-Schorey, C. ARF6-Regulated Shedding of Tumor Cell-Derived Plasma Membrane Microvesicles. *Curr Biol* 2009, *19*, 1875–1885, doi:10.1016/j.cub.2009.09.059.

95. McConnell, R.E.; Higginbotham, J.N.; Shifrin, D.A.; Tabb, D.L.; Coffey, R.J.; Tyska, M.J. The Enterocyte Microvillus Is a Vesicle-Generating Organelle. *J Cell Biol* 2009, *185*, 1285–1298, doi:10.1083/jcb.200902147.

96. Wang, T.; Gilkes, D.M.; Takano, N.; Xiang, L.; Luo, W.; Bishop, C.J.; Chaturvedi, P.; Green, J.J.; Semenza, G.L. Hypoxia-Inducible Factors and RAB22A Mediate Formation of Microvesicles That Stimulate Breast Cancer Invasion and Metastasis. *Proceedings of the National Academy of Sciences* 2014, *111*, doi:10.1073/pnas.1410041111.

97. Woodman, P.G.; Futter, C.E. Multivesicular Bodies: Co-Ordinated Progression to Maturity. *Curr Opin Cell Biol* 2008, *20*, 408–414, doi:10.1016/j.ceb.2008.04.001.

98. Krylova, S. V; Feng, D. The Machinery of Exosomes: Biogenesis, Release, and Uptake. *Int J Mol Sci* 2023, *24*, doi:10.3390/ijms24021337.

99. Mellman, I.; Yarden, Y. Endocytosis and Cancer. *Cold Spring Harb Perspect Biol* 2013, *5*, a016949–a016949, doi:10.1101/cshperspect.a016949.

100. Taguchi, T. Emerging Roles of Recycling Endosomes. *J Biochem* 2013, *153*, 505–510, doi:10.1093/jb/mvt034.

101. O'Sullivan, M.J.; Lindsay, A.J. The Endosomal Recycling Pathway—At the Crossroads of the Cell. *Int J Mol Sci* 2020, *21*, 6074, doi:10.3390/ijms21176074.

102. Kalluri, R.; LeBleu, V.S. The Biology , Function , and Biomedical Applications of Exosomes. *Science (1979)* 2020, *367*, doi:10.1126/science.aau6977.

103. Boya, P.; Reggiori, F.; Codogno, P. Emerging Regulation and Functions of Autophagy. *Nat Cell Biol* 2013, *15*, 713–720, doi:10.1038/ncb2788.

104. Fader, C.M.; Sánchez, D.; Furlán, M.; Colombo, M.I. Induction of Autophagy Promotes Fusion of Multivesicular Bodies with Autophagic Vacuoles in K562 Cells. *Traffic* 2008, *9*, 230–250, doi:10.1111/j.1600-0854.2007.00677.x.

105. Sahu, R.; Kaushik, S.; Clement, C.C.; Cannizzo, E.S.; Scharf, B.; Follenzi, A.; Potolicchio, I.; Nieves, E.; Cuervo, A.M.; Santambrogio, L. Microautophagy of Cytosolic Proteins by Late Endosomes. *Dev Cell* 2011, *20*, 131–139, doi:10.1016/j.devcel.2010.12.003.

106. Winter, V.; Hauser, M.-T. Exploring the ESCRTing Machinery in Eukaryotes. *Trends Plant Sci* 2006, *11*, 115–123, doi:10.1016/j.tplants.2006.01.008.

107. Raiborg, C.; Bache, K.G.; Gillooly, D.J.; Madshus, I.H.; Stang, E.; Stenmark, H. Hrs Sorts Ubiquitinated Proteins into Clathrin-Coated Microdomains of Early Endosomes. *Nat Cell Biol* 2002, *4*, 394–398, doi:10.1038/ncb791.

108. Wenzel, E.M.; Schultz, S.W.; Schink, K.O.; Pedersen, N.M.; Nähse, V.; Carlson, A.; Brech, A.; Stenmark, H.; Raiborg, C. Concerted ESCRT and Clathrin Recruitment Waves Define the Timing and Morphology of Intraluminal Vesicle Formation. *Nat Commun* 2018, *9*, 2932, doi:10.1038/s41467-018-05345-8.

109. Adell, M.A.Y.; Vogel, G.F.; Pakdel, M.; Müller, M.; Lindner, H.; Hess, M.W.; Teis, D. Coordinated Binding of Vps4 to ESCRT-III Drives Membrane Neck Constriction during MVB Vesicle Formation. *Journal of Cell Biology* 2014, *205*, 33–49, doi:10.1083/jcb.201310114.

110. Row, P.E.; Prior, I.A.; McCullough, J.; Clague, M.J.; Urbé, S. The Ubiquitin Isopeptidase UBPY Regulates Endosomal Ubiquitin Dynamics and Is Essential for Receptor Down-Regulation. *Journal of Biological Chemistry* 2006, *281*, 12618–12624, doi:10.1074/jbc.M512615200.

111. Baietti, M.F.; Zhang, Z.; Mortier, E.; Melchior, A.; Degeest, G.; Geeraerts, A.; Ivarsson, Y.; Depoortere, F.; Coomans, C.; Vermeiren, E.; et al. Syndecan-Syntenin-ALIX Regulates the Biogenesis of Exosomes. *Nat Cell Biol* 2012, *14*, 677–685, doi:10.1038/ncb2502.

112. Trajkovic, K.; Hsu, C.; Chiantia, S.; Rajendran, L.; Wenzel, D.; Wieland, F.; Schwille, P.; Brügger, B.; Simons, M. Ceramide Triggers Budding of Exosome Vesicles into Multivesicular Endosomes. *Science (1979)* 2008, *319*, 1244–1247, doi:10.1126/science.1153124.

113. Perez-Hernandez, D.; Gutiérrez-Vázquez, C.; Jorge, I.; López-Martín, S.; Ursa, A.; Sánchez-Madrid, F.; Vázquez, J.; Yáñez-Mó, M. The Intracellular Interactome of Tetraspanin-Enriched Microdomains Reveals Their Function as Sorting Machineries toward Exosomes. *Journal of Biological Chemistry* 2013, *288*, 11649–11661, doi:10.1074/jbc.M112.445304.

114. Kowal, J.; Arras, G.; Colombo, M.; Jouve, M.; Morath, J.P.; Primdal-Bengtson, B.; Dingli, F.; Loew, D.; Tkach, M.; Théry, C. Proteomic Comparison Defines Novel Markers to Characterize Heterogeneous Populations of Extracellular Vesicle Subtypes. *Proceedings of the National Academy of Sciences* 2016, *113*, doi:10.1073/pnas.1521230113.

115. Polo, S.; Sigismund, S.; Faretta, M.; Guidi, M.; Capua, M.R.; Bossi, G.; Chen, H.; De Camilli, P.; Di Fiore, P.P. A Single Motif Responsible for Ubiquitin Recognition and Monoubiquitination in Endocytic Proteins. *Nature* 2002, *416*, 451–455, doi:10.1038/416451a.

116. Luhtala, N.; Odorizzi, G. Bro1 Coordinates Deubiquitination in the Multivesicular Body Pathway by Recruiting Doa4 to Endosomes. *J Cell Biol* 2004, *166*, 717–729, doi:10.1083/jcb.200403139.

117. Ferreira, J.V.; da Rosa Soares, A.; Ramalho, J.; Máximo Carvalho, C.; Cardoso, M.H.; Pintado, P.; Carvalho, A.S.; Beck, H.C.; Matthiesen, R.; Zuzarte, M.; et al. LAMP2A Regulates the Loading of Proteins into Exosomes. *Sci Adv* 2022, *8*, eabm1140, doi:10.1126/sciadv.abm1140.

118. Pfeffer, S.R. Unsolved Mysteries in Membrane Traffic. *Annu Rev Biochem* 2007, *76*, 629–645, doi:10.1146/annurev.biochem.76.061705.130002.

119. Vats, S.; Galli, T. Role of SNAREs in Unconventional Secretion—Focus on the VAMP7-Dependent Secretion. *Front Cell Dev Biol* 2022, *10*, doi:10.3389/fcell.2022.884020.

120. Chaineau, M.; Danglot, L.; Galli, T. Multiple Roles of the Vesicular-SNARE TI-VAMP in Post-Golgi and Endosomal Trafficking. *FEBS Lett* 2009, *583*, 3817–3826, doi:10.1016/j.febslet.2009.10.026.

121. Pilliod, J.; Desjardins, A.; Pernègre, C.; Jamann, H.; Larochelle, C.; Fon, E.A.; Leclerc, N. Clearance of Intracellular Tau Protein from Neuronal Cells via VAMP8-Induced Secretion. *Journal of Biological Chemistry* 2020, *295*, 17827–17841, doi:10.1074/jbc.RA120.013553.

122. Ren, H.; Elgner, F.; Himmelsbach, K.; Akhras, S.; Jiang, B.; Medvedev, R.; Ploen, D.; Hildt, E. Identification of Syntaxin 4 as an Essential Factor for the Hepatitis C Virus Life Cycle. *Eur J Cell Biol* 2017, *96*, 542–552, doi:10.1016/j.ejcb.2017.06.002.

123. Yu, Z.; Shi, M.; Stewart, T.; Fernagut, P.-O.; Huang, Y.; Tian, C.; Dehay, B.; Atik, A.; Yang, D.; De Giorgi, F.; et al. Reduced Oligodendrocyte Exosome Secretion in Multiple System Atrophy Involves SNARE Dysfunction. *Brain* 2020, *143*, 1780–1797, doi:10.1093/brain/awaa110.

124. Ostrowski, M.; Carmo, N.B.; Krumeich, S.; Fanget, I.; Raposo, G.; Savina, A.; Moita, C.F.; Schauer, K.; Hume, A.N.; Freitas, R.P.; et al. Rab27a and Rab27b Control Different Steps of the Exosome Secretion Pathway. *Nat Cell Biol* 2010, *12*, 19–30, doi:10.1038/ncb2000.

125. Gurung, S.; Perocheau, D.; Touramanidou, L.; Baruteau, J. The Exosome Journey: From Biogenesis to Uptake and Intracellular Signalling. *Cell Commun Signal* 2021, *19*, 47, doi:10.1186/s12964-021-00730-1.

126. Somiya, M. Where Does the Cargo Go?: Solutions to Provide Experimental Support for the “Extracellular Vesicle Cargo Transfer Hypothesis.” *J Cell Commun Signal* 2020, *14*, 135–146, doi:10.1007/s12079-020-00552-9.

127. O’Brien, K.; Ughetto, S.; Mahjoum, S.; Nair, A. V.; Breakefield, X.O. Uptake, Functionality, and Re-Release of Extracellular Vesicle-Encapsulated Cargo. *Cell Rep* 2022, *39*, 110651, doi:10.1016/j.celrep.2022.110651.

128. Joshi, B.S.; de Beer, M.A.; Giepmans, B.N.G.; Zuhorn, I.S. Endocytosis of Extracellular Vesicles and Release of Their Cargo from Endosomes. *ACS Nano* 2020, *14*, 4444–4455, doi:10.1021/acsnano.9b10033.

129. Polanco, J.C.; Hand, G.R.; Briner, A.; Li, C.; Götz, J. Exosomes Induce Endolysosomal Permeabilization as a Gateway by Which Exosomal Tau Seeds Escape into the Cytosol. *Acta Neuropathol* 2021, *141*, 235–256, doi:10.1007/s00401-020-02254-3.

130. Morad, G.; Carman, C. V.; Hagedorn, E.J.; Perlin, J.R.; Zon, L.I.; Mustafaoglu, N.; Park, T.-E.; Ingber, D.E.; Daisy, C.C.; Moses, M.A. Tumor-Derived Extracellular Vesicles Breach the Intact Blood–Brain Barrier *via* Transcytosis. *ACS Nano* 2019, *13*, 13853–13865, doi:10.1021/acsnano.9b04397.

131. Kerr, J.F.; Wyllie, A.H.; Currie, A.R. Apoptosis: A Basic Biological Phenomenon with Wide-Ranging Implications in Tissue Kinetics. *Br J Cancer* 1972, *26*, 239–257, doi:10.1038/bjc.1972.33.

132. Elmore, S. Apoptosis: A Review of Programmed Cell Death. *Toxicol Pathol* 2007, *35*, 495–516, doi:10.1080/01926230701320337.

133. Becker, A.; Thakur, B.K.; Weiss, J.M.; Kim, H.S.; Peinado, H.; Lyden, D. Extracellular Vesicles in Cancer: Cell-to-Cell Mediators of Metastasis. *Cancer Cell* 2016, *30*, 836–848, doi:10.1016/j.ccell.2016.10.009.

134. Koliopanos, A.; Friess, H.; Kleeff, J.; Shi, X.; Liao, Q.; Pecker, I.; Vlodavsky, I.; Zimmermann, A.; Büchler, M.W. Heparanase Expression in Primary and Metastatic Pancreatic Cancer. *Cancer Res* 2001, *61*, 4655–4659.

135. Koo, T.H.; Lee, J.-J.; Kim, E.-M.; Kim, K.-W.; Kim, H. Do; Lee, J.-H. Syntenin Is Overexpressed and Promotes Cell Migration in Metastatic Human Breast and Gastric Cancer Cell Lines. *Oncogene* 2002, *21*, 4080–4088, doi:10.1038/sj.onc.1205514.

136. Liu, R.-T.; Huang, C.-C.; You, H.-L.; Chou, F.-F.; Hu, C.-C.A.; Chao, F.-P.; Chen, C.-M.; Cheng, J.-T. Overexpression of Tumor Susceptibility Gene TSG101 in Human Papillary Thyroid Carcinomas. *Oncogene* 2002, *21*, 4830–4837, doi:10.1038/sj.onc.1205612.

137. Oh, K.B.; Stanton, M.J.; West, W.W.; Todd, G.L.; Wagner, K.-U. Tsg101 Is Upregulated in a Subset of Invasive Human Breast Cancers and Its Targeted Overexpression in

Transgenic Mice Reveals Weak Oncogenic Properties for Mammary Cancer Initiation. *Oncogene* 2007, *26*, 5950–5959, doi:10.1038/sj.onc.1210401.

138. Toyoshima, M.; Tanaka, N.; Aoki, J.; Tanaka, Y.; Murata, K.; Kyuuma, M.; Kobayashi, H.; Ishii, N.; Yaegashi, N.; Sugamura, K. Inhibition of Tumor Growth and Metastasis by Depletion of Vesicular Sorting Protein Hrs: Its Regulatory Role on E-Cadherin and β-Catenin. *Cancer Res* 2007, *67*, 5162–5171, doi:10.1158/0008-5472.CAN-06-2756.

139. Guo, J.; Jayaprakash, P.; Dan, J.; Wise, P.; Jang, G.-B.; Liang, C.; Chen, M.; Woodley, D.T.; Fabbri, M.; Li, W. PRAS40 Connects Microenvironmental Stress Signaling to Exosome-Mediated Secretion. *Mol Cell Biol* 2017, *37*, doi:10.1128/MCB.00171-17.

140. Griffiths, S.; Cormier, M.; Clayton, A.; Doucette, A. Differential Proteome Analysis of Extracellular Vesicles from Breast Cancer Cell Lines by Chaperone Affinity Enrichment. *Proteomes* 2017, *5*, 25, doi:10.3390/proteomes5040025.

141. Lobb, R.J.; Hastie, M.L.; Norris, E.L.; van Amerongen, R.; Gorman, J.J.; Möller, A. Oncogenic Transformation of Lung Cells Results in Distinct Exosome Protein Profile Similar to the Cell of Origin. *Proteomics* 2017, *17*, doi:10.1002/pmic.201600432.

142. Melo, S.A.; Sugimoto, H.; O'Connell, J.T.; Kato, N.; Villanueva, A.; Vidal, A.; Qiu, L.; Vitkin, E.; Perelman, L.T.; Melo, C.A.; et al. Cancer Exosomes Perform Cell-Independent MicroRNA Biogenesis and Promote Tumorigenesis. *Cancer Cell* 2014, *26*, 707–721, doi:10.1016/j.ccell.2014.09.005.

143. Tűzesi, Á.; Kling, T.; Wenger, A.; Lunavat, T.R.; Jang, S.C.; Rydenhag, B.; Lötvall, J.; Pollard, S.M.; Danielsson, A.; Carén, H. Pediatric Brain Tumor Cells Release Exosomes with a MiRNA Repertoire That Differs from Exosomes Secreted by Normal Cells. *Oncotarget* 2017, *8*, 90164–90175, doi:10.18632/oncotarget.21621.

144. Ramteke, A.; Ting, H.; Agarwal, C.; Mateen, S.; Somasagara, R.; Hussain, A.; Graner, M.; Frederick, B.; Agarwal, R.; Deep, G. Exosomes Secreted under Hypoxia Enhance Invasiveness and Stemness of Prostate Cancer Cells by Targeting Adherens Junction Molecules. *Mol Carcinog* 2015, *54*, 554–565, doi:10.1002/mc.22124.

145. Nazarenko, I.; Rana, S.; Baumann, A.; McAlear, J.; Hellwig, A.; Trendelenburg, M.; Lochnit, G.; Preissner, K.T.; Zöller, M. Cell Surface Tetraspanin Tspan8 Contributes to Molecular Pathways of Exosome-Induced Endothelial Cell Activation. *Cancer Res* 2010, *70*, 1668–1678, doi:10.1158/0008-5472.CAN-09-2470.

146. Webber, J.; Steadman, R.; Mason, M.D.; Tabi, Z.; Clayton, A. Cancer Exosomes Trigger Fibroblast to Myofibroblast Differentiation. *Cancer Res* 2010, *70*, 9621–9630, doi:10.1158/0008-5472.CAN-10-1722.

147. Lee, K. Exosomes from Breast Cancer Cells Can Convert Adipose Tissue-Derived Mesenchymal Stem Cells into Myofibroblast-like Cells. *Int J Oncol* 2011, doi:10.3892/ijo.2011.1193.

148. Ghayad, S.E.; Rammal, G.; Ghamloush, F.; Basma, H.; Nasr, R.; Diab-Assaf, M.; Chelala, C.; Saab, R. Exosomes Derived from Embryonal and Alveolar Rhabdomyosarcoma Carry Differential MiRNA Cargo and Promote Invasion of Recipient Fibroblasts. *Sci Rep* 2016, *6*, 37088, doi:10.1038/srep37088.

149. Fahs, A.; Hussein, N.; Zalzali, H.; Ramadan, F.; Ghamloush, F.; Tamim, H.; El Homsi, M.; Badran, B.; Boulos, F.; Tawil, A.; et al. CD147 Promotes Tumorigenesis via Exosome-Mediated Signaling in Rhabdomyosarcoma. *Cells* 2022, *11*, 2267, doi:10.3390/cells11152267.

150. de Araújo, M.E.G.; Lamberti, G.; Huber, L.A. Isolation of Early and Late Endosomes by Density Gradient Centrifugation. *Cold Spring Harb Protoc* 2015, *2015*, pdb.prot083444, doi:10.1101/pdb.prot083444.

151. Bradford, M. A Rapid and Sensitive Method for the Quantitation of Microgram Quantities of Protein Utilizing the Principle of Protein-Dye Binding. *Anal Biochem* 1976, *72*, 248–254, doi:10.1006/abio.1976.9999.

152. Bright, N.A.; Gratian, M.J.; Luzio, J.P. Endocytic Delivery to Lysosomes Mediated by Concurrent Fusion and Kissing Events in Living Cells. *Current Biology* 2005, *15*, 360–365, doi:10.1016/j.cub.2005.01.049.

153. Palmulli, R. Role of CD63 in the Biogenesis and the Function of Exosomes, Paris, 2019.

154. Kalra, H.; Simpson, R.J.; Ji, H.; Aikawa, E.; Altevogt, P.; Askenase, P.; Bond, V.C.; Borràs, F.E.; Breakefield, X.; Budnik, V.; et al. Vesiclepedia: A Compendium for Extracellular Vesicles with Continuous Community Annotation. *PLoS Biol* 2012, *10*, e1001450, doi:10.1371/journal.pbio.1001450.

155. Borchers, A.-C.; Langemeyer, L.; Ungermann, C. Who's in Control? Principles of Rab GTPase Activation in Endolysosomal Membrane Trafficking and Beyond. *Journal of Cell Biology* 2021, *220*, doi:10.1083/jcb.202105120.

156. Perini, E.D.; Schaefer, R.; Stöter, M.; Kalaidzidis, Y.; Zerial, M. Mammalian <scp>CORVET</Scp> Is Required for Fusion and Conversion of Distinct Early Endosome Subpopulations. *Traffic* 2014, *15*, 1366–1389, doi:10.1111/tra.12232.

157. Tremel, S.; Ohashi, Y.; Morado, D.R.; Bertram, J.; Perisic, O.; Brandt, L.T.L.; von Wrisberg, M.-K.; Chen, Z.A.; Maslen, S.L.; Kovtun, O.; et al. Structural Basis for VPS34 Kinase Activation by Rab1 and Rab5 on Membranes. *Nat Commun* 2021, *12*, 1564, doi:10.1038/s41467-021-21695-2.

158. Langemeyer, L.; Fröhlich, F.; Ungermann, C. Rab GTPase Function in Endosome and Lysosome Biogenesis. *Trends Cell Biol* 2018, *28*, 957–970, doi:10.1016/j.tcb.2018.06.007.

159. Gruenberg, J. Life in the Lumen: The Multivesicular Endosome. *Traffic* 2020, *21*, 76–93, doi:10.1111/tra.12715.

160. Lee, K.-M.; Seo, E.-C.; Lee, J.-H.; Kim, H.-J.; Hwangbo, C. The Multifunctional Protein Syntenin-1: Regulator of Exosome Biogenesis, Cellular Function, and Tumor Progression. *Int J Mol Sci* 2023, *24*, 9418, doi:10.3390/ijms24119418.

161. Le, A.; Machesky, L. Image-Based Quantification of Macropinocytosis Using Dextran Uptake into Cultured Cells. *Bio Protoc* 2022, *12*, doi:10.21769/BioProtoc.4367.

162. Adams, S.D.; Csere, J.; D'angelo, G.; Carter, E.P.; Romao, M.; Arnandis, T.; Dodel, M.; Kocher, H.M.; Grose, R.; Raposo, G.; et al. Centrosome Amplification Mediates Small Extracellular Vesicle Secretion via Lysosome Disruption. *Current Biology* 2021, *31*, 1403-1416.e7, doi:10.1016/j.cub.2021.01.028.

163. Xie, Z.; Zhao, M.; Yan, C.; Kong, W.; Lan, F.; Narengaowa; Zhao, S.; Yang, Q.; Bai, Z.; Qing, H.; et al. Cathepsin B in Programmed Cell Death Machinery: Mechanisms of Execution and Regulatory Pathways. *Cell Death Dis* 2023, *14*, 255, doi:10.1038/s41419-023-05786-0.

164. Kabeya, Y. LC3, a Mammalian Homologue of Yeast Apg8p, Is Localized in Autophagosome Membranes after Processing. *EMBO J* 2000, *19*, 5720–5728, doi:10.1093/emboj/19.21.5720.

165. He, H.; Dang, Y.; Dai, F.; Guo, Z.; Wu, J.; She, X.; Pei, Y.; Chen, Y.; Ling, W.; Wu, C.; et al. Post-Translational Modifications of Three Members of the Human MAP1LC3 Family and Detection of a Novel Type of Modification for MAP1LC3B. *Journal of Biological Chemistry* 2003, *278*, 29278–29287, doi:10.1074/jbc.M303800200.

166. Wu, J.; Dang, Y.; Su, W.; Liu, C.; Ma, H.; Shan, Y.; Pei, Y.; Wan, B.; Guo, J.; Yu, L. Molecular Cloning and Characterization of Rat LC3A and LC3B—Two Novel Markers of Autophagosome. *Biochem Biophys Res Commun* 2006, *339*, 437–442, doi:10.1016/j.bbrc.2005.10.211.

167. Kabeya, Y.; Mizushima, N.; Yamamoto, A.; Oshitani-Okamoto, S.; Ohsumi, Y.; Yoshimori, T. LC3, GABARAP and GATE16 Localize to Autophagosomal Membrane Depending on Form-II Formation. *J Cell Sci* 2004, *117*, 2805–2812, doi:10.1242/jcs.01131.

168. Marar, C.; Starich, B.; Wirtz, D. Extracellular Vesicles in Immunomodulation and Tumor Progression. *Nat Immunol* 2021, *22*, 560–570, doi:10.1038/s41590-021-00899-0.

169. Paskeh, M.D.A.; Entezari, M.; Mirzaei, S.; Zabolian, A.; Saleki, H.; Naghdi, M.J.; Sabet, S.; Khoshbakht, M.A.; Hashemi, M.; Hushmandi, K.; et al. Emerging Role of Exosomes in Cancer Progression and Tumor Microenvironment Remodeling. *J Hematol Oncol* 2022, *15*, 83, doi:10.1186/s13045-022-01305-4.

170. Maacha, S.; Bhat, A.A.; Jimenez, L.; Raza, A.; Haris, M.; Uddin, S.; Grivel, J.-C. Extracellular Vesicles-Mediated Intercellular Communication: Roles in the Tumor Microenvironment and Anti-Cancer Drug Resistance. *Mol Cancer* 2019, *18*, 55, doi:10.1186/s12943-019-0965-7.

171. Wang, Z.; Kim, S.Y.; Tu, W.; Kim, J.; Xu, A.; Yang, Y.M.; Matsuda, M.; Reolizo, L.; Tsuchiya, T.; Billet, S.; et al. Extracellular Vesicles in Fatty Liver Promote a Metastatic Tumor Microenvironment. *Cell Metab* 2023, *35*, 1209-1226.e13, doi:10.1016/j.cmet.2023.04.013.

172. Bortot, B.; Mangogna, A.; Peacock, B.; Lees, R.; Valle, F.; Brucale, M.; Tassinari, S.; Romano, F.; Ricci, G.; Biffi, S. Platelet Activation in Ovarian Cancer Ascites: Assessment of GPIIb/IIIa and PF4 in Small Extracellular Vesicles by Nano-Flow Cytometry Analysis. *Cancers (Basel)* 2022, *14*, 4100, doi:10.3390/cancers14174100.

173. Tian, W.; Lei, N.; Zhou, J.; Chen, M.; Guo, R.; Qin, B.; Li, Y.; Chang, L. Extracellular Vesicles in Ovarian Cancer Chemoresistance, Metastasis, and Immune Evasion. *Cell Death Dis* 2022, *13*, 64, doi:10.1038/s41419-022-04510-8.

174. Komai, T.; Inoue, M.; Okamura, T.; Morita, K.; Iwasaki, Y.; Sumitomo, S.; Shoda, H.; Yamamoto, K.; Fujio, K. Transforming Growth Factor-β and Interleukin-10 Synergistically Regulate Humoral Immunity via Modulating Metabolic Signals. *Front Immunol* 2018, *9*, doi:10.3389/fimmu.2018.01364.

175. Wang, H.; Yung, M.M.H.; Ngan, H.Y.S.; Chan, K.K.L.; Chan, D.W. The Impact of the Tumor Microenvironment on Macrophage Polarization in Cancer Metastatic Progression. *Int J Mol Sci* 2021, *22*, 6560, doi:10.3390/ijms22126560.

176. Lawson, C.; Kovacs, D.; Finding, E.; Ulfelder, E.; Luis-Fuentes, V. Extracellular Vesicles: Evolutionarily Conserved Mediators of Intercellular Communication. *Yale J Biol Med* 2017, *90*, 481–491.

177. Dixson, A.C.; Dawson, T.R.; Di Vizio, D.; Weaver, A.M. Context-Specific Regulation of Extracellular Vesicle Biogenesis and Cargo Selection. *Nat Rev Mol Cell Biol* 2023, *24*, 454–476, doi:10.1038/s41580-023-00576-0.

178. Minciacchi, V.R.; Freeman, M.R.; Di Vizio, D. Extracellular Vesicles in Cancer: Exosomes, Microvesicles and the Emerging Role of Large Oncosomes. *Semin Cell Dev Biol* 2015, *40*, 41–51, doi:10.1016/j.semcdb.2015.02.010.

179. Welsh, J.A.; Goberdhan, D.C.I.; O'Driscoll, L.; Buzas, E.I.; Blenkiron, C.; Bussolati, B.; Cai, H.; Di Vizio, D.; Driedonks, T.A.P.; Erdbrügger, U.; et al. Minimal Information for Studies of Extracellular Vesicles (MISEV2023): From Basic to Advanced Approaches. *J Extracell Vesicles* 2024, *13*, doi:10.1002/jev2.12404.

180. Xu, S.; Cao, B.; Xuan, G.; Xu, S.; An, Z.; Zhu, C.; Li, L.; Tang, C. Function and Regulation of Rab GTPases in Cancers. *Cell Biol Toxicol* 2024, *40*, 28, doi:10.1007/s10565-024-09866-5.

181. Liu, W.-R.; Jin, L.; Tian, M.-X.; Jiang, X.-F.; Yang, L.-X.; Ding, Z.-B.; Shen, Y.-H.; Peng, Y.-F.; Gao, D.-M.; Zhou, J.; et al. Caveolin-1 Promotes Tumor Growth and Metastasis via Autophagy Inhibition in Hepatocellular Carcinoma. *Clin Res Hepatol Gastroenterol* 2016, *40*, 169–178, doi:10.1016/j.clinre.2015.06.017.

182. Zhang, X.; Ramírez, C.M.; Aryal, B.; Madrigal-Matute, J.; Liu, X.; Diaz, A.; Torrecilla-Parra, M.; Suárez, Y.; Cuervo, A.M.; Sessa, W.C.; et al. Cav-1 (Caveolin-1) Deficiency Increases Autophagy in the Endothelium and Attenuates Vascular Inflammation and Atherosclerosis. *Arterioscler Thromb Vasc Biol* 2020, *40*, 1510–1522, doi:10.1161/ATVBAHA.120.314291.

183. Yoshii, S.R.; Mizushima, N. Monitoring and Measuring Autophagy. *Int J Mol Sci* 2017, *18*, 1865, doi:10.3390/ijms18091865.

184. Visnovitz, T.; Lenzinger, D.; Koncz, A.; Vizi, P.M.; Bárkai, T.; Vukman, K. V; Galinsoga, A.; Németh, K.; Fletcher, K.; Komlósi, Z.I.; et al. A "Torn Bag Mechanism" of Small Extracellular Vesicle Release via Limiting Membrane Rupture of e *n Bloc* Released Amphisomes (Amphiectosomes) 2024.